

# Exploring the Biotechnological potential of freshwater Diatoms

A Dissertation for

Course code and Course Title: GBT-651 Dissertation

Submitted in partial fulfilment of Master of Science Degree  
in Biotechnology

by

**VEDHA DAMODAR DESSAI**

Roll Number: 22P0470025

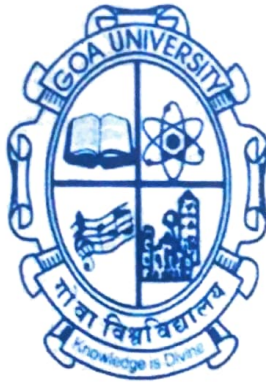
ABC ID: 867-366-134-891

PRN: 201902531

Under the Guidance of

**Ms. SNESHA BHOMKAR**

School of Biological Sciences and Biotechnology  
M.Sc. Biotechnology



Goa University

Date: 8 April 2024



Examined by:

*Sanib*  
8/4/24

*sanitaherkar*  
8/4/24

*Sanib*

*San*

*San*  
8/4/24

*Anayankar*  
8/4/24

*Bhomkar*  
8/4/24

Seal of the School

*[Signature]*

**DECLARATION BY STUDENT**

I hereby declare that the data presented in this Dissertation report entitled, “Exploring the Biotechnological potential of freshwater Diatoms” is based on the results of investigations carried out by me in the Discipline Biotechnology at the School of Biological Sciences and Biotechnology, Goa University under the Supervision of Ms. Snesha Bhomkar and the same has not been submitted elsewhere for the award of a degree or diploma by me. Further, I understand that Goa University or its authorities will not be responsible for the correctness of observations / experimental or other findings given the dissertation.

I hereby authorize the University authorities to upload this dissertation on the dissertation repository or anywhere else as the UGC regulations demand and make it available to any one as needed.

*Dessai*

Ms. Vedha Damodar Dessai

22P04700025

M.Sc. Biotechnology

School of Biological Sciences and Biotechnology

Date: 08 April 2024

Place: Goa University

**COMPLETION CERTIFICATE**

This is to certify that the dissertation report “**Exploring the Biotechnological potential of freshwater Diatoms**” is a bonafide work carried out by Ms. Vedha Damodar Dessai under my supervision in partial fulfilment of the requirements for the award of the degree of Masters of Science in the Discipline of Biotechnology at the School of Biological Sciences and Biotechnology, Goa University.

Ms. Snesha Bhomkar

Biotechnology

Date:

08 April 2024

Prof. Bernard F. Rodrigues

Sr. Professor and Dean

School stamp

School of Biological Sciences and Biotechnology

Date: 8/4/24

Place: Goa University

**Dean of School of Biological Sciences  
& Biotechnology  
Goa University, Goa-403206**



## CONTENT

<b>Chapters</b>	<b>Particulars</b>	<b>Page No.</b>
	Preface	v
	Acknowledgement	vi
	List of Tables	viii
	List of Figures	ix
	Abbreviations	xv
	Abstract	xvi
1.	<b>Introduction</b>	1
	1.1 Background	1
	1.2 Aim and Objectives	8
	1.3 Hypothesis	9
	1.4 Scope	10
2.	<b>Literature Review</b>	13
3.	<b>Methodology</b>	19
4.	<b>Result</b>	30
5.	<b>Discussion</b>	67
	Conclusion	72
	Future Prospects	73
	References	74
	Appendices	92

## **PREFACE**

When I first stumbled upon freshwater diatoms, it wasn't because of some grand scientific pursuit. I was just intrigued by these tiny creatures living their lives underwater. There was something mesmerizing about their shapes and colours, something that made me want to learn more.

As I read more, I stumbled upon something truly remarkable—the potential of these diatoms in Biotechnology. One of the most promising avenues I discovered was their application in drug delivery systems. Imagine harnessing the natural efficiency of diatoms to transport medication to precisely where it's needed in the body, revolutionizing the way we treat diseases.

But that's not all. These tiny organisms also hold tremendous promise in the realm of agricultural wastewater treatment. By leveraging their unique properties, we could develop sustainable solutions to purify contaminated water, ensuring the health of our ecosystems and communities.

So, as you journey through these pages, remember that what may have started as a personal fascination has evolved into a scientific pursuit with real-world implications. Join me as we delve into the fascinating world of freshwater diatoms, discovering their potential to revolutionize fields like drug delivery and agricultural wastewater treatment. This work stands as a contribution to the ongoing development of these exciting fields, where nature and technology collaborate to address our most pressing challenges.

## **ACKNOWLEDGEMENT**

Firstly, I'd like to extend my sincere gratitude to Sr. Prof. Bernard F. Rodrigues, the Dean of the School of Biological Sciences and Biotechnology, Goa University, to Dr. Savita Kerkar, Former Dean, School of Biological Sciences and Biotechnology, to Sr. Prof. Sanjeev Ghadi, Vice Dean (Academics), School of Biological Sciences and Biotechnology, to Prof. S. Krishnan, Vice Dean (Research), School of Biological Sciences and Biotechnology, and to Dr. Meghanath Prabhu, the Programme Director of Biotechnology Discipline, for providing the necessary facilities for carrying out this research work.

I'm deeply grateful to Ms. Snesha Bhomkar, my guide, for her unwavering support, and invaluable guidance. Her encouragement and wisdom not only shaped this dissertation but also enriched my academic journey in profound ways. Thank you for being an exceptional mentor.

I'm thankful to the Biotechnology faculty, Dr. Sanika Samant, Ms. Dviti Mapari, Dr. Samantha Fernandes D'mello, and Ms. Snigdha Mayenkar, for sharing their wisdom and expertise throughout my Master's degree.

Special thanks to our non-teaching staff—Sanjana ma'am, Sandhya ma'am, Jaya ma'am, Serrao Sir, Sameer Sir, and Ashish Sir—for their invaluable assistance in meeting project requirements. I also thank Dr. Nitin S. Sawant, the Program Director of Zoology, for granting access to the inverted

microscope in their esteemed laboratory, and research scholar Ms. Sasha Viegas for her assistance with it.

I extend my thanks to Dr. Prachi Torney and Mr. Prajot Chari from the School of Chemical Sciences, Goa University, for their aid in conducting FTIR analysis, and to Dr. M. G. Lanjewar for aiding in SEM analysis.

To my fellow classmates, Sejal, Hari, Tanmay, Sushant, Kaushiki, Samradni, Varisha, Anurag, and Ankit, your unwavering support has been my beacon of light, guiding me through every step. My heartfelt love and gratitude are yours.

I extend my heartfelt gratitude to my family for their steadfast support and encouragement during the completion of this dissertation. Their unwavering belief in me has been a source of strength throughout this journey. Additionally, I am grateful to God for enabling me to overcome challenges and reach this significant milestone. Their presence, prayers, and blessings have been invaluable to me during this process.

## List of Tables

<b>Table No.</b>	<b>Description</b>	<b>Page No.</b>
1	Frequency of phytoplankton enumerated per mL of concentrated sample after fixation with Lugol's Iodine in Carambolim I, Carambolim II, Batim I, Batim II	44
2	Diversity indices (Simpson and Shannon) for different sampling sites (Carambolim I, Carambolim II, Batim I, and Batim II)	45
3	The loading capacity and encapsulation efficiency observed for each sample.	55

### List of Figures

<b>Fig. No.</b>	<b>Description</b>	<b>Page No.</b>
1	Images depicting the sampling site: Carambolim lake, sampled on 15 September 2023 (left) and on 27 October 2023 (right).	30
2	Images depicting the sampling site: Batim lake, sampled on 8 December 2023 (left) and on 18 January 2024 (right)	30
3	A bar graph showing the estimated concentration of dissolved oxygen present in the water samples.	31
4	Test tubes depicting a series of standards of Silicates prepared with Sodium Hexafluorosilicate.	31
5	A line graph depicting absorbance at 810 nm for a series of standard concentrations of Silicate.	32
6	A bar graph showing the variation of silicate content in the different samples.	32
7	Test tubes depicting a series of standards of phosphates prepared with potassium dihydrogen orthophosphate.	33
8	A calibration line depicting absorbance at 880 nm for a series of standard concentrations of Phosphate.	33
9	A bar graph showing the variation of phosphate content in the different samples.	33
10	Test tubes depicting a series of standards of Nitrite prepared with Sodium Nitrite.	34
11	A line graph showing absorbance at 540 nm for a series of standard concentrations of nitrites.	34
12	A bar graph depicting the variation in concentration of nitrites in the water samples.	34

13	Image of a refractometer, showing the salinity of the water sample to be 0 parts per thousand.	35
14	A pie chart depicting the diversity of phytoplankton observed in Carambolim I	35
15	A pie chart depicting the diversity of phytoplankton observed in Carambolim II	36
16	A pie chart depicting the diversity of phytoplankton observed in Batim I	37
17	A pie chart depicting the diversity of phytoplankton observed in Batim II	37
18	a. <i>Trachelomonas</i> sp., b. <i>Syctonema</i> sp., c. <i>Phacus</i> sp., d. <i>Closterium gracile</i>	38
19	a. <i>Navicula</i> sp., b. <i>Navicula</i> sp., c. <i>Mastogloia</i> sp., d. <i>Closterium</i> sp., e. <i>Nitzschia</i> sp., f. <i>Coelastrum</i> sp., g. <i>Xanthodinium eckertii</i> sp., h. <i>Micrasterias</i> sp.	38
20	<i>Synedra</i> sp., b. <i>Cyclotella</i> sp., c. <i>Pinnularia</i> sp., d. <i>Navicula</i> sp., e. <i>Aulacosiera</i> sp., f. <i>Cymbella</i> sp., g. <i>Melosira</i> sp., h. <i>Navicula</i> sp.	38
21	a. <i>Staurodesmus</i> sp., b. <i>Cosmarium</i> sp., c. <i>Dimorphococcus</i> sp., d. <i>Comasiella</i> sp., e. <i>Scenedesmus</i> sp., f. <i>Tertrallantos lagerheimii</i> , g. <i>Kirchneriella</i> sp., h. <i>Ankistrodesmus</i> sp.	39
22	a. <i>Leptolyngbya</i> sp., b. <i>Phormidium</i> sp., c. <i>Anabaena</i> sp., d. <i>Oscillatoria</i> sp., e. <i>Pseudoanabaena</i> sp., f. <i>Merismopedia</i> sp., g. <i>Staurastrum</i> sp., h. <i>Pediastrum</i> sp.	39
23	a. <i>Phacus</i> sp., b. <i>Planktothrix</i> sp., c. <i>Monoraphidium</i> sp., d. <i>Lepocinclis pseudoovum</i> , e. <i>Euglena</i> sp., f. <i>Peridinium</i> sp., g. <i>Haplotaenium</i> sp., h. <i>Staurodesmus</i> sp.	39
24	<i>Nitzschia</i> sp. isolated from Carambolim I, observed under Infinity inverted microscope at 400x magnification.	42

25	<i>Navicula</i> sp. isolated from Carambolim II, observed under an inverted microscope at 400x magnification.	42
26	<i>Cymbella</i> sp. isolated from Batim I, observed under an inverted microscope at 400x magnification.	42
27	<i>Pinnularia</i> sp. isolated from Batim II, observed under an inverted microscope at 400x magnification.	43
28	A line graph depicting the growth curve of <i>Navicula</i> sp., enumerated using a hemocytometer and expressed as number of cells x 10 <sup>5</sup> cells/mL.	43
29	A line graph depicting the growth curve of <i>Nitzschia</i> sp., enumerated using a hemocytometer and expressed as number of cells x 10 <sup>5</sup> cells/mL.	44
30	A line graph depicting the growth curve of <i>Cymbella</i> sp., enumerated using a hemocytometer and expressed as number of cells x 10 <sup>5</sup> cells/mL.	44
31	A line graph depicting the growth curve of <i>Pinnularia</i> sp., enumerated using a hemocytometer and expressed as number of cells x 10 <sup>5</sup> cells/mL.	45
32	Light microscopy image of <i>Navicula</i> frustules (left) and <i>Cymbella</i> frustule (right) after acid and hydrogen peroxide treatment, observed at 200x magnification.	46
33	Light microscopy image of <i>Pinnularia</i> frustule (left) and <i>Nitzschia</i> frustules (right) after acid and hydrogen peroxide treatment, observed at 200x magnification.	46
34	SEM image of acid and hydrogen peroxide treated <i>Nitzschia</i> frustule.	46

35	SEM image of acid and hydrogen peroxide treated <i>Cymbella</i> frustule.	47
36	SEM image of acid and hydrogen peroxide treated <i>Navicula</i> frustules.	47
37	SEM image of acid and hydrogen peroxide treated <i>Pinnularia</i> frustules.	47
38	FT-IR spectrum of <i>Cymbella</i> frustules after treating with APTES	48
39	FT-IR spectrum of <i>Nitzschia</i> frustules after treating with APTES	48
40	FT-IR spectrum of <i>Navicula</i> frustules after treating with APTES	49
41	FT-IR spectrum of <i>Pinnularia</i> frustules after treating with APTES	49
42	A calibration curve for Indomethacin created using acetone as the solvent.	50
43	Cumulative percentage release of indomethacin from <i>Nitzschia</i> frustules over a period 24 hours.	52
44	Cumulative percentage release of indomethacin from <i>Navicula</i> frustules over a period 48 hours.	52
45	Cumulative percentage release of indomethacin from <i>Cymbella</i> frustules over a period 72 hours.	53
46	Cumulative percentage release of indomethacin from <i>Pinnularia</i> frustules over a period 24 hours.	53
47	Fine powder of fertiliser granules used for producing simulated wastewater.	54
48	Set of flasks of <i>Pinnularia</i> (top) and <i>Cymbella</i> (bottom) prepared for analysing the potential of diatoms for agricultural wastewater treatment.	54
49	Set of flasks of <i>Navicula</i> prepared for analysing the potential of diatoms for agricultural wastewater treatment.	54
50	A line graph showing variation in phosphate content in the simulated wastewater over the	55

	period of inoculation for the test and control flasks of <i>Navicula</i> .	
51	A line graph showing variation in phosphate content in the simulated wastewater over the period of inoculation for the test and control flasks of <i>Cymbella</i> .	55
52	A line graph showing variation in phosphate content in the simulated wastewater over the period of inoculation for the test and control flasks of <i>Pinnularia</i> .	56
53	Test tubes depicting a series of standards of Ammonia prepared with Ammonium chloride.	57
54	A graph depicting the calibration curve prepared for estimation of ammonia.	58
55	A line graph showing variation in ammonia content in the simulated wastewater over the period of inoculation for the test and control flasks of <i>Navicula</i> .	58
56	A line graph showing variation in ammonia content in the simulated wastewater over the period of inoculation for the test and control flasks of <i>Cymbella</i> .	59
57	A line graph showing variation in ammonia content in the simulated wastewater over the period of inoculation for the test and control flasks of <i>Pinnularia</i> .	59
58	A line graph showing variation in nitrite content in the simulated wastewater over the period of inoculation for the test and control flasks of <i>Navicula</i> .	60
59	A line graph showing variation in nitrite content in the simulated wastewater over the period of inoculation for the test and control flasks of <i>Cymbella</i> .	61

60	A line graph showing variation in nitrite content in the simulated wastewater over the period of inoculation for the test and control flasks of <i>Pinnularia</i> .	61
61	A line graph showing variation in nitrate content in the simulated wastewater over the period of inoculation for the test and control flasks of <i>Navicula</i> .	62
62	A line graph showing variation in nitrate content in the simulated wastewater over the period of inoculation for the test and control flasks of <i>Cymbella</i>	63
63	A line graph showing variation in nitrate content in the simulated wastewater over the period of inoculation for the test and control flasks of <i>Pinnularia</i>	63
64	A line graph showing the comparison of cell density of <i>Navicula</i> between the flask control flask, containing just f/2 medium and the culture, and the test flasks containing f/2 supplemented simulated wastewater & plainly wastewater without f/2, over a 16-day incubation period.	69
65	A line graph showing the comparison of cell density of <i>Cymbella</i> between the flask control flask, containing just f/2 medium and the culture, and the test flasks containing f/2 supplemented simulated wastewater & plainly wastewater without f/2, over a 16-day incubation period.	70
66	A line graph showing the comparison of cell density of <i>Pinnularia</i> between the flask control flask, containing just f/2 medium and the culture, and the test flasks containing f/2 supplemented simulated wastewater & plainly wastewater without f/2, over a 16-day incubation period.	70

## **ABBREVIATIONS**

- °C - Degree Celsius
- mL – Milli litre
- mg – Milli gram
- g- Gram
- L - litre
- % - Percentage
- Hr – Hour
- Min – Minutes
- Abs – Absorbance
- SEM- Scanning electron microscope
- FTIR- Fourier-transform infrared spectroscopy
- LC – Loading capacity
- EE – Encapsulation Efficiency
- DO – Dissolved Oxygen
- $\mu$ M – Micromolar
- Conc. – Concentration

## **ABSTRACT**

Diatoms, the unicellular algae with intricate silica frustules, possess unique properties like high surface area and high productivity, making them promising for biotechnological applications like drug delivery systems and for agricultural wastewater treatment. Four diatom monocultures, *Nitzschia*, *Navicula*, *Cymbella* and *Pinnularia*, isolated from freshwater lakes of Goa, were cleaned using acid-hydrogen peroxide mixture and subjected to functionalisation, followed by characterisation of their frustules using SEM and FT-IR analysis. While *Pinnularia* showed highest drug loading capacity of 26.3% with indomethacin, a model drug, the release occurred in 24 hours, with an initial burst release of 75.17% occurring after one hour. *Cymbella*, with a comparatively lower loading capacity (12.1%) showed a burst release of 73% after the first two hours, followed by sustained release over the next 72 hours. The isolates tested for their ability to reduce nutrient concentration in simulated wastewater showed significant results when supplemented with f/2 components, with *Navicula* sp. emerging as the best candidate, being able to reduce phosphate content by 58.75%, ammonia content by 49.48% and nitrate content by 28.3%.

# CHAPTER – I

# *1. INTRODUCTION*

# 1. Introduction

## 1.1. Background

Wetlands serve an indispensable function in controlling the Earth's climate, managing the global water cycle, preserving biodiversity, and ensuring the well-being of humanity (Gardner & Davidson, 2011; Townsend, 1993). These are ecosystems characterised by the presence of water, either seasonally or permanently and support a wide range of lifeforms, including microscopic phytoplankton (Xu, Chen, Yang, Jiang, & Zhang, 2020)

Phytoplankton are photosynthetic organisms that form the basis of aquatic food webs (Kilham & Hecky, 1988). They encompass various types including diatoms, dinoflagellates, cyanobacteria, coccolithophores, and green algae (Sournia, 1978). Chlorophyta (green algae) and Cyanophyta (cyanobacteria) exhibit a strong affinity for freshwater environments, with a notable decline in species diversity within these groups observed in marine ecosystems. Conversely, coccolithophores, characteristic of marine plankton, are rarely found in freshwater (Kilham & Hecky, 1988). Diatoms, belonging to the class Bacillariophyta, are ubiquitous eukaryotes found in both freshwater and marine environments. These organisms exhibit a photosynthetic mode of nutrition and are typically characterised by a golden-brown pigmentation due to the presence of fucoxanthin (Beakes, Canter, & Jaworski, 1988).

## **Freshwater Diatoms**

Studying the variety of freshwater diatoms in relation to their environment has become increasingly important. This research not only helps us understand these ecosystems but could also lead to the discovery of valuable diatom species. These species could then be commercially cultivated as beneficial biological resources (Arumugham, Joseph, P M, Nooruddin, & Subramani, 2023). Diatoms have been noted to offer biotechnological potential due to the ample amorphous silica in their cell walls, providing benefits like high surface area and biocompatibility (Sardo, Orefice, Balzano, Barra, & Romano, 2021).

### **A. Diatom Biosilica:**

The cell walls of diatoms, called frustules, feature highly porous, nanopatterned surfaces with strong mechanical properties. The siliceous parts, initially protected by organic matter (proteins and carbohydrates) in water, can be effectively cleaned through acid/oxidation methods to yield nanostructured biosilica shells used in applications like photonics, molecular separation, biosensing, and drug delivery microsystems (Jiang et al., 2013). Originally diatomite, a fossil source of diatoms, was used for obtaining biosilica (Sheng et al., 2009). However, living diatoms are a more sustainable and superior source of frustules compared to diatomite. Fossils are finite, while living diatoms offer higher-quality frustules with better surface area and integrity. Subterranean diatomite deposits can damage frustule structures, and various diatoms provide a wider range of frustule shapes.

Additionally, diatomite usually contains a mix of species, making it difficult to isolate specific frustule characteristics (Gurel and Yildiz 2007).

### **Purification of Frustules:**

Over the years, researchers have employed several methods, used alone or in combination, to purify the frustules from the cultured diatoms. The effectiveness of these techniques in removing the organic matter vary from one genus to the next, depending on fragility, structural complexity and size (Wang, Cai, Jiang, Jiang, & Zhang, 2012).

### **Application in Drug Delivery:**

Nanoporous silica materials, like mesoporous silica and porous silicon, are vital in nanomedicine for drug delivery due to their high surface area, stability, and biocompatibility. The commonly employed silica variants, such as Mobil Oil Corporation's Mobile Composition of Matter No.-41 (MCM-41) and Santa Barbara University's Santa Barbara Amorphous-15 (SBA-15), exhibit a pore size range from 2 to 50 nanometers. However, their synthesis is expensive and involves toxic chemicals. Biosilica from the diatom frustules offer a natural alternative (Simovic, Ghouchi-Eskandar, Moom Sinn, Losic, & A. Prestidge, 2011; McInnes & Voelcker, 2009).

The commercialization of mesoporous silica nanoparticles (MSN) faces limitations due to issues such as cytotoxicity and challenges in scale-up, stemming from the use of various toxic substances in their production. In contrast, diatom biosilica, naturally synthesised from diatoms, offers a more

environmentally friendly manufacturing process, involving minimal chemicals, primarily H<sub>2</sub>O<sub>2</sub>, in the purification process. Cytotoxicity tests demonstrate that diatom biosilica exhibits low cytotoxicity and high biocompatibility. On the other hand, the synthesis of MSN involves the use of toxic substances like surfactants, methanol, or expensive silica materials as templates e.g., MCM-41 or SBA-15 (Lim et al., 2023).

Drug release from cleansed diatom frustules is controlled by altering pore size, facilitating controlled and prolonged release by reducing pore size. Surface modifications offer the ability to regulate drug loading and release strategies (Bariana, Aw, Kurkuri, & Losic, 2013; Ukmar et al., 2011) The use of organosilanes (Aw, Bariana, Yu, Addai-Mensah, & Losic, 2012), dopamine-iron oxide (Losic et al., 2010) or electrostatic attachment of Graphene oxide sheets (Kumeria et al., 2013), are some surface modifications that have been incorporated earlier for aiding in drug delivery.

In this study we have cultured the isolated diatoms from the samples, and purified them using acid-hydrogen peroxide treatment. The purified frustules are then subjected to various analyses for determination of their characteristics and then tested for their potential in drug delivery by carrying out drug release studies.

## **B. Nutrient composition of agricultural wastewater & mechanisms of uptake:**

Excessive water usage in agriculture, municipalities, and industries results in large volumes of wastewater, containing high levels of nutrients like nitrogen and phosphorus. This contributes to eutrophication in lakes, posing a serious environmental problem that has become more widespread since the mid-20th century (Dodds et al., 2008). Studies have proven the use of microalgae to be efficient in reducing the amount of nutrients such as phosphorus and nitrogen from a wide range of wastewater (Sturm & Lamer, 2011; Zhou et al., 2012), including agricultural wastewater (Mulbry, Kondrad, Pizarro, & Kebede-Westhead, 2008).

Wastewater from animal farms typically contains nitrogen-to-phosphorus ratio of 2-8; approximately half of the nitrogen exists as ammonium, while the other half is in the form of organic nitrogen (Ashekuzzaman, Forrestal, Richards, & Fenton, 2019; Rayne & Aula, 2020). These excess soil nutrients result in heightened nutrient runoff, ultimately causing eutrophication in water bodies (Dodds et al., 2008).

Organic nitrogen originates from various inorganic sources such as nitrate ( $\text{NO}_3^-$ ), nitrite ( $\text{NO}_2^-$ ), nitric acid ( $\text{HNO}_3$ ), ammonium ( $\text{NH}_4^+$ ), ammonia ( $\text{NH}_3$ ), and nitrogen gas ( $\text{N}_2$ ). Microalgae are instrumental in converting inorganic nitrogen into its organic form through assimilation. Nitrate and nitrite undergo reduction within the microalgae with the assistance of nitrate reductase and nitrite reductase, respectively (Barsanti & Gualtieri, 2014;

Collos & Slawyk, 1980). Ammonium is removed through cell metabolism and ammonia stripping, where high pH and temperature levels can lead to significant ammonia volatilization (García, Mujeriego, & Hernández-Mariné, 2000). Inorganic phosphates are crucial for microalgae cell growth. Phosphorus is incorporated into organic compounds through phosphorylation, requiring energy input and involving ATP generation from ADP (Martínez, Jiménez, & El Yousfi, 1999).

### **Use of phytoplankton in nutrient removal**

*Chlorella*, a member of the green algae belonging to the Chlorophyta phylum, has been extensively studied and demonstrated effectiveness in nutrient removal. Studies by Aslan & Kapdan (2006), Kong et al. (2009), and Wang et al. (2010) reported nitrogen and phosphorus removal efficiencies ranging from 8% to 100%.

Similarly, *Scenedesmus*, another chlorophyte, has been evaluated for its potential to reduce nutrient concentrations in high-nutrient wastewater. *S. dimorphus* and *S. obliquus* have shown notable reductions in nutrient content in industrial wastewater (González, Cañizares, & Baena, 1997) and municipal wastewater (Lavoie & de la Noüe, 1985), respectively.

Moreover, certain cyanobacteria such as *Arthrospira*, *Synechococcus*, *Oscillatoria*, and *Phormidium* have made significant contributions to nutrient reduction in wastewater, as indicated by research conducted by Cai, Park, & Li (2013).

**Role of diatoms in nutrient removal:**

Diatoms exhibit a notably higher nutrient uptake rate compared to other algal groups, attributed to their substantial nutrient storage capacity (Litchman, Klausmeier, Miller, Schofield, & Falkowski, 2006). This advantage allows them to surpass other algae in productivity, even under nutrient-rich conditions (Amano, Takahashi, & Machida, 2011). In wastewater systems, benthic diatoms form robust symbiotic relationships with bacteria, enhancing nutrient removal efficiency and oxygen production (Wilkie, 2002).

The potential of freshwater diatoms in mitigating nutrient pollution within agricultural wastewater remains a relatively underexplored domain. Consequently, this study also aims to address this research gap by investigating the impact of diatoms on agricultural wastewater and their capacity to reduce nutrient concentrations.

## **1.2. Aim and Objectives:**

Aim: Exploring the biotechnological potential of freshwater diatoms.

Objectives:

1. Study of physico-chemical parameters of water samples.
2. Assessment of phytoplankton Diversity.
3. To isolate Diatoms from fresh water lakes in Goa
4. Determining the potential of isolated diatoms as a delivery system.
5. Evaluating the potential of the isolated diatoms for treating agricultural wastewater.

### **1.3. Research Hypothesis**

Following the purification of their frustules, the diatoms isolated are anticipated to display substantial potential as a delivery system due to their unique structural characteristics and biocompatibility. It is hypothesised that these purified diatom isolates will exhibit efficient encapsulation properties, making them suitable for the controlled release of therapeutic agents or other bioactive compounds.

Furthermore, it is hypothesized that these diatom isolates will demonstrate the ability to effectively reduce the concentration of nutrients in agricultural wastewater. This hypothesis is based on the known capacity of diatoms to uptake and assimilate nutrients from their surrounding environment. Through their metabolic processes, the diatoms may actively remove excess nutrients, such as nitrogen and phosphorus, thereby mitigating the environmental impact of agricultural runoff and promoting water quality improvement.

## 1.4 Scope

This research project is designed to explore the entire process involved in harnessing the potential of diatoms for various applications, with a particular focus on drug delivery and agricultural wastewater treatment. The scope encompasses several key stages, beginning with the isolation of diatoms from freshwater ecosystems. Through meticulous isolation techniques, diverse diatom species will be collected and cultured in laboratory settings, followed by purification of their frustules to extract pristine silica structures for potential drug delivery. Surface functionalization techniques will modify frustule properties, enabling efficient drug loading and controlled release. In-vitro studies will evaluate release kinetics, guiding further optimization of the delivery system. This research also explores diatoms' potential for agricultural wastewater treatment. It involves inoculating diatom cultures into simulated wastewater containing agricultural nutrients. Diatoms' effectiveness in nutrient removal will be monitored to quantify their capability in reducing nutrient concentrations. Overall, the study aims to advance diatoms' applications in drug delivery and wastewater treatment, offering sustainable solutions to environmental and healthcare challenges through interdisciplinary approaches.

# **CHAPTER – II**

## *2. REVIEW OF LITERATURE*

## **2. REVIEW OF LITERATURE**

### **2.1. Potential of Diatoms as a Delivery system:**

#### **2.1.1. Frustule Cleaning/Purification:**

A study described a method for characterising diatom frustules on a mica surface. The frustules were baked at either 400 or 800°C for 2 hours. Baking at 400°C successfully removed organic components, allowing clear observation of the frustule patterns. Baking at 800°C resulted in increased nanopore size, and the appearance of large holes at the end of frustules, visualized using Scanning Electron Microscopy. (Umemura et al., 2008).

To purify diatom biosilica frustules, a two-step method involving acid cleaning and baking was used by Jiang et.al (2013). This process effectively removed organic and inorganic impurities. The best results were achieved with a 10-15% HCl wash followed by heating to 600°C over 6 hours. The native frustule structure remained intact, resulting in dry frustules with over 90% SiO<sub>2</sub> by weight and a significant surface area of 48.47 m<sup>2</sup> g<sup>-1</sup>.

Qi, Wang and Cheng (2016) successfully produced pure biosilica from marine diatoms *Nitzschia closterium* and *Thalassiosira* using acid washing and thermal treatment. The optimal method involved a 2% HCl wash for 0.5 hours followed by baking at 600°C for another 0.5 hours, leading to a significant increase in Si content. Based on the mass removal efficiency, *N. closterium* and *Thalassiosira* were subjected to 2% HCl acid wash treatment and baking at 600°C, following which the silica content was determined. *N.*

*closterium* showed a SiO<sub>2</sub> content of 92.23% and *Thalassiosira* showed a SiO<sub>2</sub> content of 91.52%. Both biosilica types exhibited amorphous silica morphologies, with *N. closterium* biosilica having micropores and fibers, and *Thalassiosira* biosilica featuring a hierarchical skeleton with mesopores. The resulting biosilica possessed a highly porous surface structure.

Silanol groups (-Si-OH) offer reactive sites that can be easily modified with diverse functional moieties, providing precise control over surface properties. They react with silane coupling agents, enabling covalent attachment of functional groups, introducing specific chemical functionalities that impact interactions with drugs, cells, and tissues. These groups are valuable for controlled drug loading and release, with the surface functionalization creating binding sites for drugs, allowing modulation of release kinetics based on the nature of functional groups and their interactions with drug molecules (Maher, Kumeria, Aw, & Losic, 2018).

Saad et al. (2020) investigated how various cleaning techniques affect the dissolution of diatom frustules. The findings suggested that rigorous cleaning methods like oxygen plasma etching can alter the three-dimensional structure of the SiO<sub>2</sub> framework and the presence of silanol groups.

Extended exposure to acid wash and heating treatments can eventually impact the structures of frustules. Acidic solutions such as HCl and H<sub>2</sub>SO<sub>4</sub> are utilized at concentrations that selectively dissolve organic matter without causing corrosion to the frustules. Critical parameters like acid concentration,

temperature, and contact time are fine-tuned to minimize any adverse effects on the biosilica structure. The dissolution of biosilica in acid occurs at a relatively slow pace. While there may be slight etching on the biosilica's surface, the overall structure remains largely unaltered due to the slower reaction kinetics between the acid and biosilica compared to the reaction with organic matter (Sardo et al., 2021).

### **2.1.2. Surface Functionalization & Drug Release Studies:**

In 2010, Losic et al. pioneered the use of diatoms, specifically *Aulacoseira* sp., for drug delivery. They modified diatom surfaces with dopamine and iron oxide nanoparticles, enabling precise drug release control and magnetic guidance. The process involved one-step magnetization through electrostatic attraction, and initial tests with the poorly water-soluble drug indomethacin showed a drug loading capacity of  $0.28 \pm 0.05$  g/g. Drug release occurred in two phases, with 60% released in the first 6 hours and the remaining 40% released over two weeks.

In another study, the same drug was used to determine drug release by diatom frustules without surface modification. Indomethacin was loaded into diatom pores, resulting in a rapid 65-70% drug release in the first 2 hours, likely due to weak bonds with the silica surface. Slow release over two weeks occurred from drug stored in the diatom micropores, following zero-order kinetics. Surface modification of diatoms was achieved using various organosilanes, such as APTES, 16-phosphonic-hexadecanoic acid phosphonic acids, and 2-

carboxyethyl-phosphonic acid, for desired functionality (Aw, Bariana, Yu, Addai-Mensah, & Losic, 2012)

Organosilanes are used to influence the hydrophilic and hydrophobic properties of diatom surfaces. The presence of functional groups leads to changes in drug release profiles (6-15 days) and drug loading capacity (15-24%). Studies with hydrophobic (indomethacin) and hydrophilic (gentamicin) drugs showed that hydrophobic drug loading is improved on hydrophilic surfaces like epoxy-rich GPTMS and APTES, resulting in higher drug loading and controlled release (Aw, Bariana, Yu, Addai-Mensah, & Losic, 2012).

Cicco et al., in 2015, investigated the use of chemically modified diatom biosilica for bone cell growth and drug delivery. They employed purified *Thalassiosira weissflogi* diatoms functionalized with TEMPO, a potent reactive oxygen species scavenger. Ciprofloxacin served as the model drug, exhibiting both initial burst release and controlled release over 7 days. This approach shows promise for infection treatment in orthopaedic and dental surgery, mitigating inflammatory side effects, and enhancing bone cell adhesion and proliferation.

In a different study, the diatomite surface was bioengineered to enhance cellular uptake and optimize drug delivery. They modified the diatom with APTES and tested it in a phosphate saline buffer at pH 7.4. This modified diatom was then used to assess drug loading and release properties with the

poorly water-soluble drug Sorafenib. The study revealed a significant increase in drug loading capacity, leading to improved drug release, reduced toxicity, and enhanced cellular uptake (Terracciano et al., 2015). Drug release in biosilica-based systems typically involves two distinct phases: an initial rapid release phase, attributed to the detachment of drug molecules weakly bound to the frustule surface, and a subsequent slow-release phase, resulting from the delivery of drugs from the internal pore structure of diatom frustules (Maher et al., 2018).

A novel microfluidic encapsulation method was developed and compared with traditional methods, offering faster encapsulation within minutes. The rich OH groups in frustules facilitated intramolecular interactions for encapsulation. Optimal conditions were found to be 2 minutes resident time in the microfluidic device and an isorhamnetin concentration of 20 µg/mL. Drug release exhibited an initial burst release, releasing 48.26% of the drug in the first hour, followed by complete release within 3 hours (Mancera-Andrade et al., 2019).

## **2.2. Potential for treatment of wastewater.**

Abou-Shanab, Ji, Kim, Paeng, & Jeon (2013) investigated the efficacy of six microalgal species, *Ourococcus multisporus*, *Nitzschia cf. pusilla*, *Chlamydomonas mexicana*, *Scenedesmus obliquus*, *Chlorella vulgaris*, and *Micractinium reisseri* in integrating piggy wastewater treatment with biodiesel production. *C. mexicana* demonstrated the highest nitrogen (62%), phosphorus (28%), and inorganic carbon (29%) removal rates.

*Chlorella vulgaris* effectively removed nutrients from concentrated cattle farm wastewater, with removal rates of 62.30% for chemical oxygen demand (COD), 81.16% for NH<sub>4</sub>-N, and 85.29% for total phosphorus (TP). Two-stage processes further enhanced nutrient removal, achieving efficiencies of 91.24%-92.17% for COD, 83.16% - 94.27% for NH<sub>4</sub>-N, and 90.98%-94.41% for TP within 3-5 days (Lv et al., 2018).

Urban wastewater from a eutrophic was used to cultivate a diatom algae consortium and assess the effects of silica and trace metal enrichment on growth, nutrient removal, and lipid production. The consortium was dominated by the diatoms, *Achnantheidium exiguum*, *Navicula crytocephala*, *Cymbella tugidula*, *Navicula gracilis*, and *Pleurosigma elongatum*. Nano-silica-based micronutrient mixture Nualgi was employed to optimize diatom growth, resulting in impressive reductions of 95.1% for nitrogen and 88.9% for phosphorus (Marella, Parine, & Tiwari, 2018).

Another research assessed *Phaeodactylum tricornutum*, a marine diatom, for its ability to remove nutrients and produce biodiesel using various ratios of mixed municipal wastewater (MW) and seawater (SW) as growth media. Results showed high nutrient removal efficiency at MW: SW ratios of 1:1 and 2:1, with COD, total nitrogen, TP, and NH<sub>3</sub>-N removal ranging from 76.9% to 97.0% (Wang et al., 2019).

# **CHAPTER - III**

### *3. MATERIALS & METHODOLOGY*

### **3. METHODOLOGY**

#### **3.1. Sampling:**

##### **3.1.1. Study areas:**

Two notified wetlands of Goa, Carambolim Lake, and Batim Lake were selected for the purpose of this study. Situated at 15.4888° N, 73.9279° E, Carambolim Lake is a man-made wetland along the side of the Mandovi River in central Goa, India, A unique regional wetland, this area serves as a haven for a diverse and abundant bird population. The wetland's rich ecosystem provides a variety of food sources, including algae, grasses, insects, crustaceans, mollusks, and fish (Shanbhag, Walia, & Borges, 2001). Batim lake is a natural wetland, located at 15.4495° N, 73.8956° E. It provides an array of ecosystem services including buffering communities from extreme events such as floods and storms, acting as a sink for sediments, groundwater recharge, fisheries, etc. (Goa State Biodiversity Board, 2020).

##### **3.1.2. Sampling strategy for diversity and isolation of phytoplankton:**

Each site was sampled twice, the consecutive sampling being done approximately a month after the first in order to increase the sample size.

For the purpose of isolation of diatoms, 750 ml of surface water sample was collected, and was subjected to filtration through a 20 µm mesh. To the filtered water sample, as per Guillard and Ryther 1962, components of the f/2 media were added in appropriate amounts and the sample bottles were

incubated in artificial light conditions (16 h light period, followed by 8 h of darkness).

Another batch of the water sample, 500 ml, post filtration was fixed using 4 ml of Lugol's Iodine for determining the phytoplankton diversity.

### **3.2. Study of physico-chemical parameters of water sample:**

#### **3.2.1. Determination of Dissolved Oxygen:**

In an amber coloured stoppered bottle, 250ml of the water sample was collected, ensuring that no bubbling occurred, for the purpose of determination of dissolved oxygen (DO). Immediately, 1 ml of Winkler's A and 1 ml of Winkler's B reagents were added, and the bottle was sealed, shaken and allowed to settle.

To the fixed DO bottle, 1 ml of concentrated H<sub>2</sub>SO<sub>4</sub> was added and the bottle was shaken thoroughly to dissolve the precipitate. 50 ml of this sample was then titrated against Na<sub>2</sub>S<sub>2</sub>O<sub>3</sub> using starch as an indicator (Grasshoff, Kremling, Ehrhardt, & Anderson, 1999). The amount of dissolved oxygen present in the water sample was then evaluated using the following formula:

$$\text{Amount of DO in water sample} = \text{Total volume of Na}_2\text{S}_2\text{O}_3 \text{ used} * \text{Normality of Na}_2\text{S}_2\text{O}_3 * 1000 * \text{Equivalent weight of oxygen} / \text{Volume of the sample}$$

### **3.2.2. Estimation of Inorganic Silicates:**

25 mL of the water sample was taken in a plastic test tube, to which 1 mL of Molybdate reagent was added. The tube was allowed to stand for 10-20 mins, after which 1 mL of Oxalic acid was added followed by addition of 0.5 mL of Ascorbic acid and the tube was incubated at room temperature (RT) for 30 mins to allow a blue colour to develop. The absorbance was then measured at 810 nm. The values were compared with a sodium hexafluoro-silicate ( $\text{Na}_2\text{SiF}_6$ ) standard (Grasshoff et al., 1999).

### **3.2.3. Estimation of Inorganic Phosphates:**

To 25 mL of water sample, 0.5 mL of Ascorbic acid and 0.5 mL of Mixed Reagent were added. The tubes were mixed well and kept at RT for 10 mins to allow the development of a blue colour, followed by determination of absorbance at 880 nm against a standard curve prepared from potassium dihydrogen orthophosphate ( $\text{KH}_2\text{PO}_4$ ) (Grasshoff et al., 1999).

### **3.2.4. Estimation of Nitrites:**

To 25 mL of water sample, 0.5 mL of sulphanilamide solution was added and incubated briefly for a period of 5 mins. After incubation, 0.5 mL of N-(1-Naphthyl) ethylenediamine dihydrochloride solution was added and the sample was incubated in dark for 15 mins to allow a pink colour to develop. The absorbance of the samples was measured at a wavelength of 540 nm. The concentration of the test samples was then estimated using a calibration curve generated with a standard sodium nitrite ( $\text{NaNO}_2$ ) solution (Grasshoff et al., 1999).

### **3.2.5. Determination of Salinity:**

The salinity of the water sample was determined using a refractometer and expressed as parts per thousand.

### **3.3. Assessment of phytoplankton diversity:**

The filtered water sample fixed with Lugol's Iodine was allowed to settle for 48 hours. The sediment layer formed was then used for determining the diversity of phytoplankton present originally in the sample. Without disturbing the sediment layer, the water from the top was carefully siphoned off and reduced to approximately 20 ml. With the help of a micropipette, 1 ml of this sample was added into a Sedgewick-Rafter counting chamber and the number and types of phytoplankton were enumerated, followed by analysis of diversity indices, namely: Shannon (H), and Simpson (D) index using software PAST.

### **3.4. Isolation, Culturing and Identification of Diatoms:**

The technique of micromanipulation was adopted for carrying out isolation of the freshwater diatoms. The filtered sample incubated after addition of Guillard's f/2 medium was added into a six-well plate. The sample was visualised using Olympus CK2 inverted microscope, and individual diatom cells were located and aspirated into the next well. The process was repeated every day until there was no growth of other contaminating phytoplankton observed in the well plate.

The identification of the isolates was done using Hasle & Tomas (1997) key.

Following isolation, the diatom culture was inoculated into a 50 mL Erlenmeyer flask. Daily aliquots of 10  $\mu$ L were withdrawn from the culture and enumerated using a haemocytometer to monitor the growth curve of the isolated diatom strain.

### **3.5. Determining the potential of the isolated diatoms as a delivery system:**

#### **3.5.1. Frustule Purification:**

In order to clean the frustules, a protocol elaborated by Mancera-Andrade et al., (2019), with slight modification, was used. An eight-day old diatom culture incubated in Guillard's f/2 medium was centrifuged at 4000 rpm for 15 minutes. The cells were washed with distilled water twice to eradicate traces of the medium. Afterward, the cell pellet was placed in a 50 mL centrifuge tube, to which 30 mL of 30% hydrogen peroxide ( $H_2O_2$ ) and 0.2 mL of 37% hydrochloric acid (HCl) were added. Subsequently, the tubes were incubated at 90°C for 3 hours. Following this, the HCl/ $H_2O_2$  solution was removed using a pipette, and the pellet was washed with distilled water twice. The cleaned frustules were visualised using light microscopy and stored in methanol at <4°C until further use.

#### **3.5.2. Scanning Electron Microscopy (SEM) analysis:**

The frustules were visualised by SEM using a ZEISS EVO 18 Scanning Electron Microscope to determine the efficiency of the cleaning technique. Using a micropipette, a small amount of the frustules was transferred to a 1

cm x 1 cm glass slide. Sample prepared was using a protocol modified from Seaborn & Wolny (2000). The sample was fixed overnight using 2.5% glutaraldehyde, following which a series of dehydration steps were carried out with ethanol (25%, 50%, 75%, 95% and 100%).

### **3.5.3. Surface Functionalization:**

0.1 g of dry frustules was suspended in 3 ml of toluene under vacuum. To this mixture, 1 ml of distilled water was added, and it was stirred for 1–2 hours at ambient temperature to facilitate the dispersion of water throughout the solid–liquid suspension. Following this, 170  $\mu$ l of APTES [(3-aminopropyl) triethoxysilane] was added, and the mixture was refluxed for 3 hours. The frustules were then collected by filtration after thorough rinsing with isopropanol and subsequently dried in a vacuum desiccator under ambient conditions before subjecting to FT-IR analysis using Bruker alpha 2 model; the data was further analysed using Origin 8 software (Bariana, Aw, Kurkuri, & Losic, 2013).

### **3.5.4. Drug Loading:**

0.5 mL of ethanol was added to 10 mg of frustules to facilitate efficient pore wetting and improve drug encapsulation inside the pores. 8 mg of indomethacin drug was dissolved in 2 mL ethanol, yielding a concentration of 4 mg/ml and the mixture was sonicated for 1 h in order to achieve a homogenous solution, followed by repeated drop-wise loading into the ethanol wetted frustule sample and allowed to evaporate (Aw, Simovic, Yu, Addai-Mensah, & Losic, 2012).

The loading capacity was evaluated by determining the amount of drug adsorbed onto the diatom frustules by a desorption procedure adapted from Mancera-Andrade et al. (2019), wherein the drug loaded frustules were centrifuged with distilled water to remove non-absorbed drug, followed by addition of acetone to desorb the attached indomethacin. The supernatant upon centrifugation was collected, and the concentration of the loaded drug was assessed based on a standard calibration curve of indomethacin prepared using acetone as the diluent.

#### **3.5.5. In-vitro release studies:**

In the first stage of this experiment, a Simulated Colonic Fluid (SCF) was prepared. This solution contained 0.2 g/L potassium chloride, 8 g/L sodium chloride, 0.24 g/L potassium phosphate monobasic, and 1.44 g/L sodium phosphate dibasic. The final pH of the SCF was adjusted to 7. Next, 30 mL of the prepared SCF was transferred to a 125 mL Erlenmeyer flask. A sample containing drug-loaded frustules was then added to the flask. The entire mixture was incubated under agitation conditions for 24 hours at 37°C and 50 rpm. To monitor the release of the drug throughout the experiment, samples were collected every 30 mins for the first three hours, followed by at 6 hours, 18 hours and 24 hours of incubation. At each hour point, 700 µL of the solution was removed from the flask. To maintain a constant volume within the flask, an equal volume (700 µL) of fresh SCF was then added back. The concentration of the released drug in the collected samples was

subsequently determined using spectrophotometry at 320 nm using SCF as the diluent for the standard (Mancera- Andrade et al., 2019).

### **3.6. Evaluating the ability of the isolated diatoms to treat wastewater:**

#### **3.6.1. Production of Simulated Agricultural Wastewater:**

In order to determine whether the isolates obtained showed the potential for accumulating nutrients, simulated agricultural wastewater was formulated using locally obtained fertiliser granules. Pre-treatment involved crushing the granules into a fine powder with the aid of a mortar pestle and drying this powder for 2 hr at 80°C in a hot air oven to eradicate moisture. The powder was dissolved in sterile distilled water (0.1 g per 100 mL) according to the sets analysed in the study. These sets were categorized as follows:

A. Fertilizer + Culture + f/2 medium (TEST)

B. Culture + f/2 medium (CONTROL)

C. Culture only (CONTROL)

D. Fertilizer only (CONTROL)

E. Fertilizer + culture (TEST)

The flasks were then labeled as follows:

- NA, NB, NC, ND, & NE for *Navicula* sp.

- CA, CB, CC, CD, & CE for *Cymbella* sp.

- PA, PB, PC, PD, & PE for *Pinnularia* sp.

### **3.6.2. Analysis of nutrient composition:**

On Day 0, Day 8, and Day 16, water samples from each set of flasks were withdrawn and filtered through a 0.45µm filter paper. The filtered water was then tested for the following contents: Total Nitrogen (Nitrate, Nitrite, and Ammonia), Phosphorus, and the Relative Percent Reduction for each nutrient compared with Control (fertiliser only). ANOVA-Single Factor test was carried out to determine if there was a significant difference between the control and the test flasks at a significance level of  $p = 0.05$ . Additionally, on Day 4, Day 8, Day 12 and Day 16 of incubation, an aliquot of 0.9 mL was taken from each flask and fixed using 0.1mL Lugol's Iodine to determine the cell density.

#### **3.6.2.1. Estimation of Phosphate content:**

The variation in the phosphate content of the simulated wastewater was analysed using ascorbic acid reagent by a protocol mentioned in section 3.2.3. (Grasshoff et al., 1999).

#### **3.6.2.2. Estimation of Ammonia:**

20 ml of water sample was taken, to which 1 mL of sodium potassium tartarate solution was added to avoid cloudiness in the tube. This was followed by addition of 1 mL of Nessler's reagent and subsequent incubation for 20 mins before absorbance was measured at a wavelength of 420 nm. A

calibration curve was prepared using ammonium chloride ( $\text{NH}_4\text{Cl}$ ) for determination of unknown concentration (ASTM, 2008).

#### **3.7.2.3. Estimation of Nitrite:**

The differences in the nitrite content of the wastewater were determined by a protocol given by Grasshoff et al., (1999) described in section 3.2.4.

#### **3.7.2.4. Estimation of Nitrate:**

A column filled with copperized cadmium granules and equilibrated using ammonium chloride buffer was used to reduce the nitrate present in the samples to nitrite. Subsequently, the estimation follows the protocol mentioned in section 3.2.4. (Grasshoff et al., 1999).

#### **3.7.3. Determination of cell density:**

0.1 mL of the agricultural wastewater sample was fixed with 0.9 mL of Lugol's Iodine on day 4, day 8, day 12, and day 16 of incubation to determine the cell density of the culture using a haemocytometer (Hindarti & Larasati, 2019). Only the flasks wherein the diatom culture were inoculated (A, B & E) were used for checking cell density. The flasks belonging to set C were not used as due to lack of any growth medium, there would be no increase in the cell density.

# **CHAPTER – IV**

## *4. RESULTS & DISCUSSION*

## 4. RESULTS

### 4.1. Sampling

Carambolim lake was sampled on 15 September 2023 and 27 October 2023; hereafter the samples are referred to as Carambolim I and Carambolim II, respectively. The sampling was conducted in Batim lake on 8 December 2023 and 18 January 2023, hereafter referred to as Batim I and Batim II, respectively.

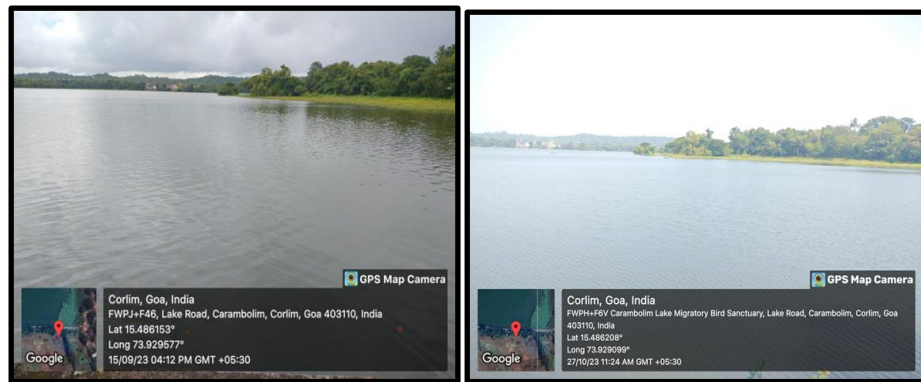


Fig. 1. Images depicting the sampling site: Carambolim lake, sampled on 15 September 2023 (left) and on 27 October 2023 (right).

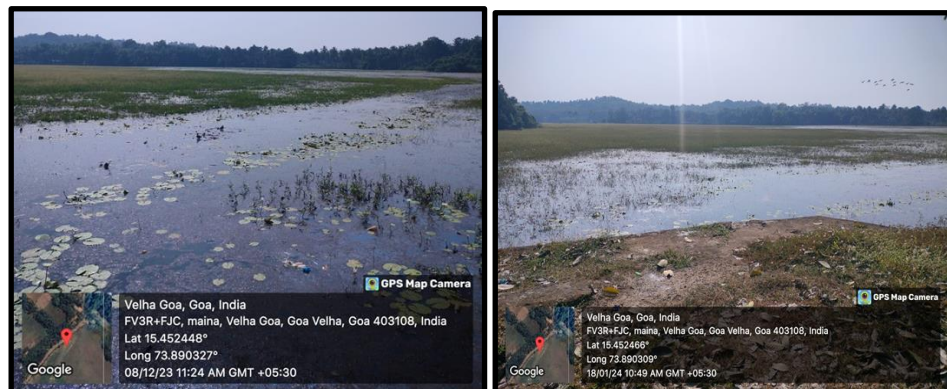


Fig. 2. Images depicting the sampling site: Batim lake, sampled on 8 December 2023 (left) and on 18 January 2024 (right)

## 4.2. Study of physico-chemical parameters of water sample:

### 4.2.1. Determination of Dissolved Oxygen:

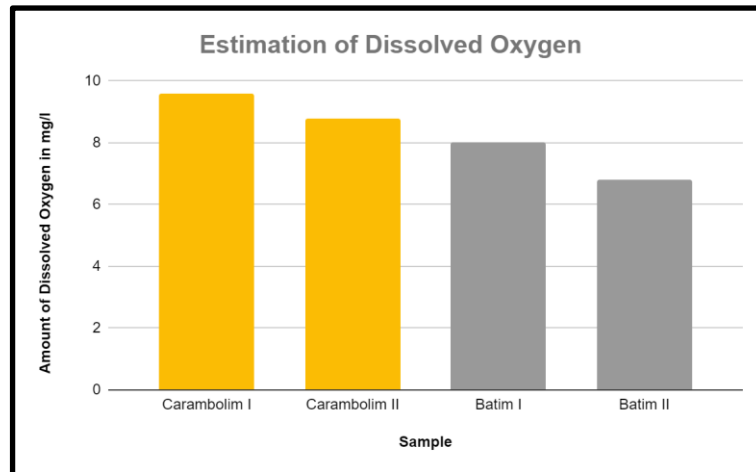


Fig. 3. A bar graph showing the estimated concentration of dissolved oxygen present in the water samples.

The content of dissolved oxygen present in the sample Carambolim I, Carambolim II, Batim I, and Batim II were found to be 9.6 mg/L, 8.8 mg/L, 8 mg/L and 6.8 mg/L, respectively

### 4.2.2. Estimation of Inorganic Silicates:

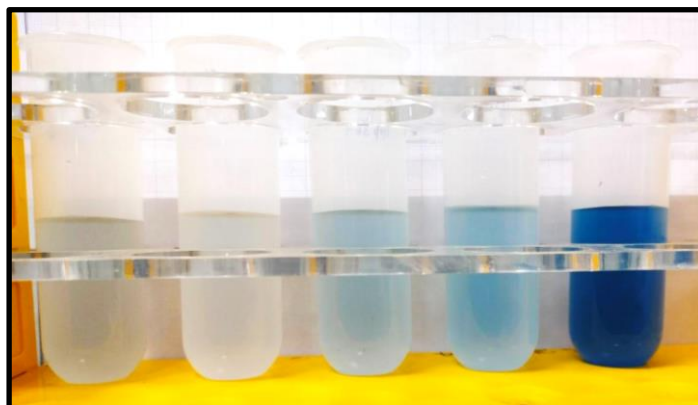


Fig. 4. Test tubes depicting a series of standards of Silicates prepared with Sodium Hexafluorosilicate.

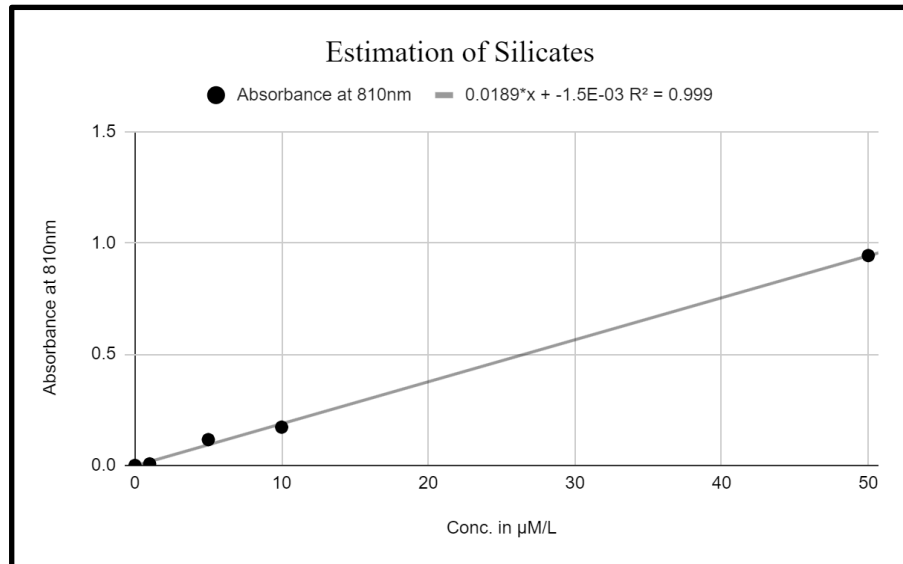


Fig. 5. A line graph depicting absorbance at 810 nm for a series of standard concentrations of Silicate.

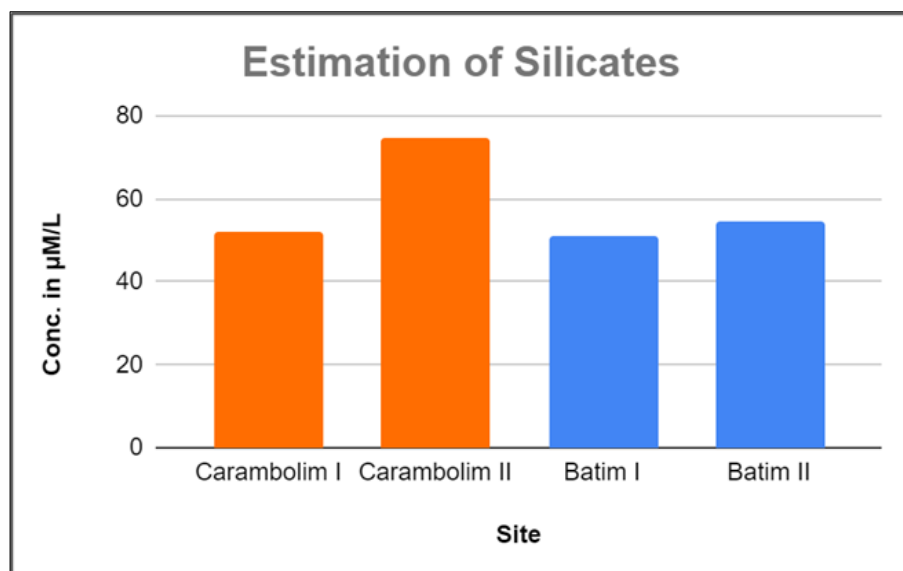


Fig. 6. A bar graph showing the variation of silicate content in the different samples.

Based on the calibration curve, the silicate concentrations in the water samples were estimated and found to be  $51.95 \mu\text{M/L}$ ,  $74.44 \mu\text{M/L}$ ,  $51.21 \mu\text{M/L}$  and  $54.33 \mu\text{M/L}$  for Carambolim I, Carambolim II, Batim I and Batim II, respectively.

### 4.2.3. Estimation of Inorganic Phosphates:



Fig. 7. Test tubes depicting a series of standards of phosphates prepared with potassium dihydrogen orthophosphate.

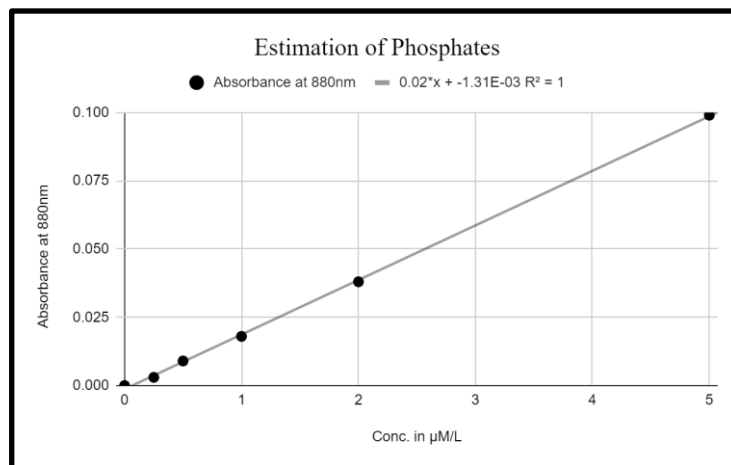


Fig. 8. A calibration line depicting absorbance at 880 nm for a series of standard concentrations of Phosphate.

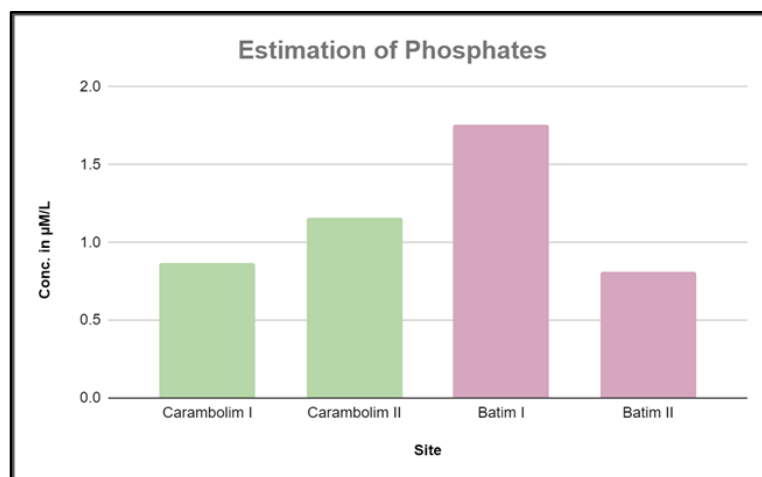


Fig. 9. A bar graph showing the variation of phosphate content in the different samples.

The concentration of inorganic phosphates was evaluated based on the standard calibration curve and were determined to be 0.86  $\mu\text{M/L}$ , 1.16  $\mu\text{M/L}$ , 1.7  $\mu\text{M/L}$ , 0.81  $\mu\text{M/L}$  for Carambolim I, Carambolim II, Batim I and Batim II, respectively.

#### 4.2.4. Estimation of Nitrites:

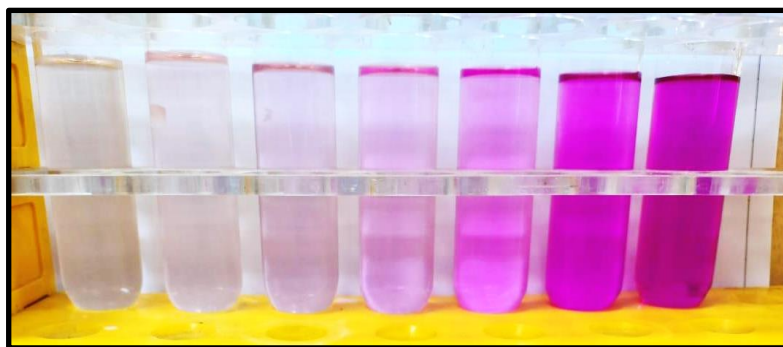


Fig. 10. Test tubes depicting a series of standards of Nitrite prepared with Sodium Nitrite.

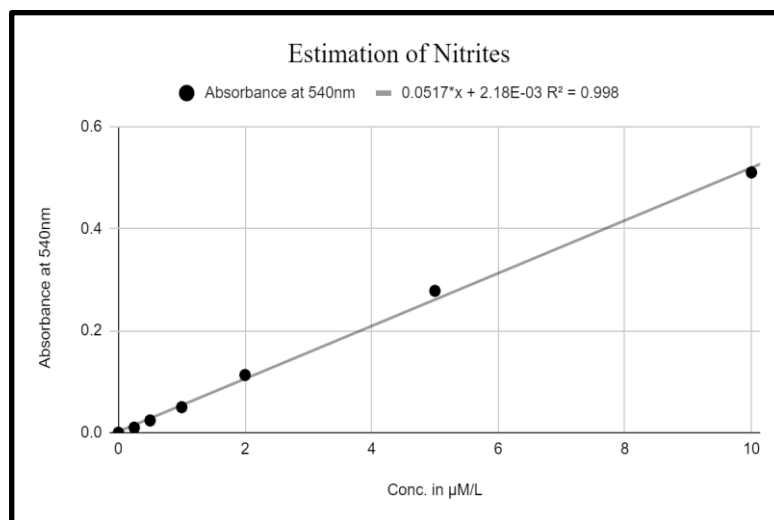


Fig. 11. A line graph showing absorbance at 540 nm for a series of standard concentrations of nitrites.

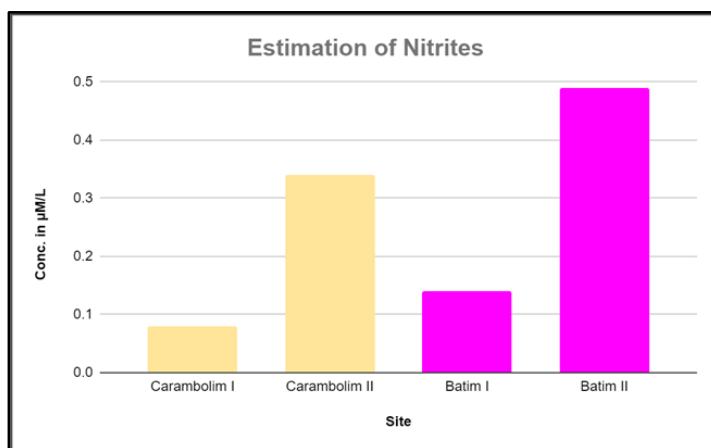


Fig. 12. A bar graph depicting the variation in concentration of nitrites in the water samples.

The absorbance values obtained for the water samples were compared with the standard and the concentration of nitrites present was determined. Carambolim I had  $0.079 \mu\text{M/L}$  of nitrite, Carambolim II contained  $0.34 \mu\text{M/L}$ , for Batim I it was found to be  $0.14 \mu\text{M/L}$ , and Batim II had the highest concentration of nitrite among the rest at  $0.49 \mu\text{M/L}$ .

#### 4.2.5. Determination of Salinity:

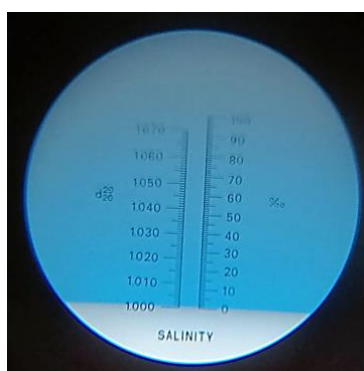


Fig. 13. Image of a refractometer, showing the salinity of the water sample to be 0 parts per thousand.

The salinity was measured using a refractometer and was found to be 0 parts per thousand for each of the samples, establishing them as freshwater.

#### 4.3. Assessment of Phytoplankton diversity:

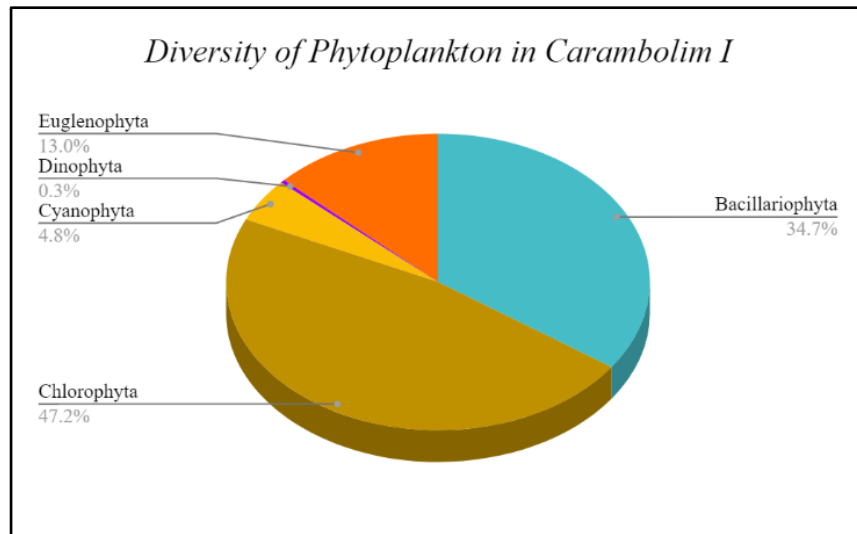


Fig. 14. A pie chart depicting the diversity of phytoplankton observed in Carambolim I

In the freshwater ecosystem of Carambolim I, Chlorophyta (green algae) emerged as the predominant group, comprising 47.2% of the total phytoplankton observed. Following closely behind were diatoms, classified under the division Bacillariophyta, constituting 34.7% of the phytoplankton community. Euglenophytes contributed 13% to the overall composition, while Cyanophyta, or cyanobacteria, made up 4.8%. Dinophyta, a minor component, represented only 0.3% of the total phytoplankton population in the area.

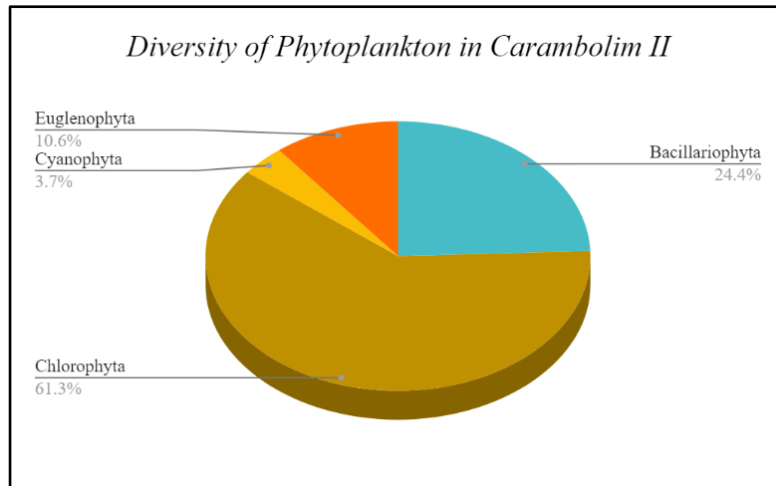


Fig. 15. A pie chart depicting the diversity of phytoplankton observed in Carambolim II

In Carambolim II, a comparable phytoplankton composition was observed, similar to that of Carambolim I. Chlorophyta maintained its dominance, representing a significant portion at 61.3% of the total phytoplankton enumerated. Bacillariophyta, while slightly lower in abundance, still constituted a substantial 24.4%. Euglenophyta contributed 10.6% to the overall composition, with Cyanophyta comprising the remaining 3.7%. Notably, dinoflagellates were absent from the fixed sample collected in Carambolim II.

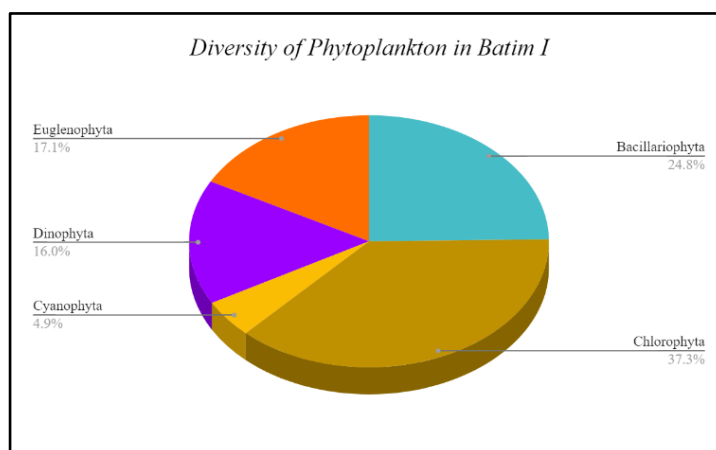


Fig. 16. A pie chart depicting the diversity of phytoplankton observed in Batim I

In the initial Batim sample, Chlorophyta emerged as the dominant phylum, constituting 37.3% of the phytoplankton population. Bacillariophyta followed closely behind, representing 24.8% of the observed community. Euglenophyta contributed significantly with 17.1% abundance. Dinophyta, primarily represented by the dinoflagellate *Peridinium* sp., made up 16% of the phytoplankton assemblage. Cyanophyta, although a minority, still contributed 4.9% to the overall composition.

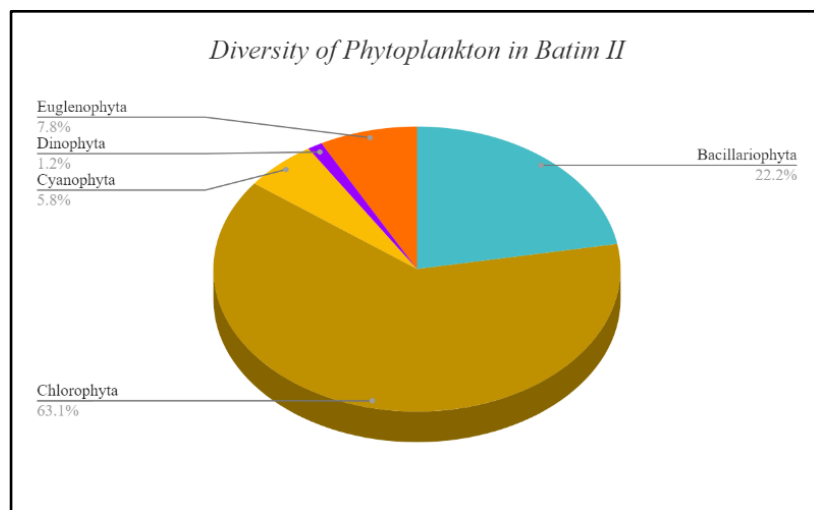


Fig. 17. A pie chart depicting the diversity of phytoplankton observed in Batim I

In the Batim II sample, Chlorophyta emerged as the dominant phylum, accounting for a substantial 63.1% of the total phytoplankton population. Bacillariophyta represented a significant portion, comprising 22.2% of the observed community. Following closely, Euglenophyta emerged as the next abundant group, contributing 7.8% to the overall composition; Cyanophyta constituted 5.8% of the phytoplankton population. Dinophyta, although in lower abundance, were still present, representing 1.2% of the enumerated community.

A detailed list of the phytoplankton observed in the fixed water samples can be found in Table 1.



Fig. 18. a. *Trachelomonas* sp., b. *Syctonema* sp., c. *Phacus* sp., d. *Closterium gracile*

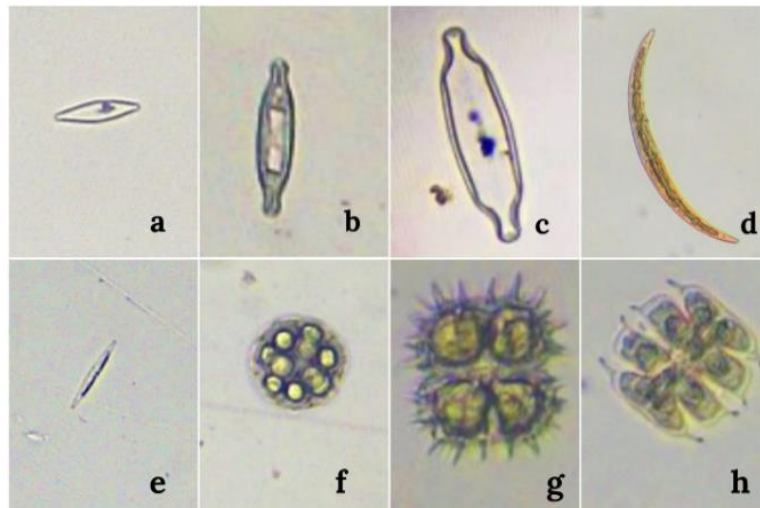


Fig. 19. a. *Navicula* sp., b. *Navicula* sp., c. *Mastogloia* sp., d. *Closterium* sp., e. *Nitzschia* sp., f. *Coelastrum* sp., g. *Xanthodinium eckertii* sp., h. *Micrasterias* sp.



Fig. 20. a. *Synedra* sp., b. *Cyclotella* sp., c. *Pinnularia* sp., d. *Navicula* sp., e. *Aulacosiera* sp., f. *Cymbella* sp., g. *Melosira* sp., h. *Navicula* sp.

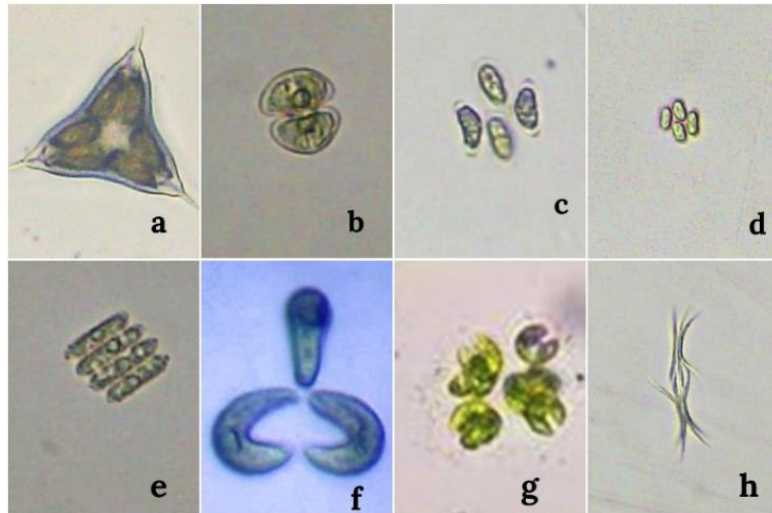


Fig. 21. a. *Staurodesmus* sp., b. *Cosmarium* sp., c. *Dimorphococcus* sp., d. *Comasiella* sp., e. *Scenedesmus* sp., f. *Tertrallantos lagerheimii*, g. *Kirchneriella* sp., h. *Ankistrodesmus* sp.

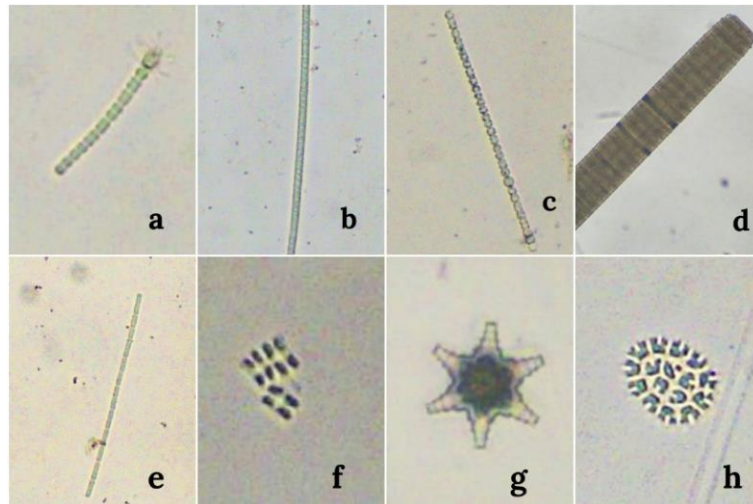


Fig. 22. a. *Leptolyngbya* sp., b. *Phormidium* sp., c. *Anabaena* sp., d. *Oscillatoria* sp., e. *Pseudoanabaena* sp., f. *Merismopedia* sp., g. *Staurastrum* sp., h. *Pediastrum* sp.

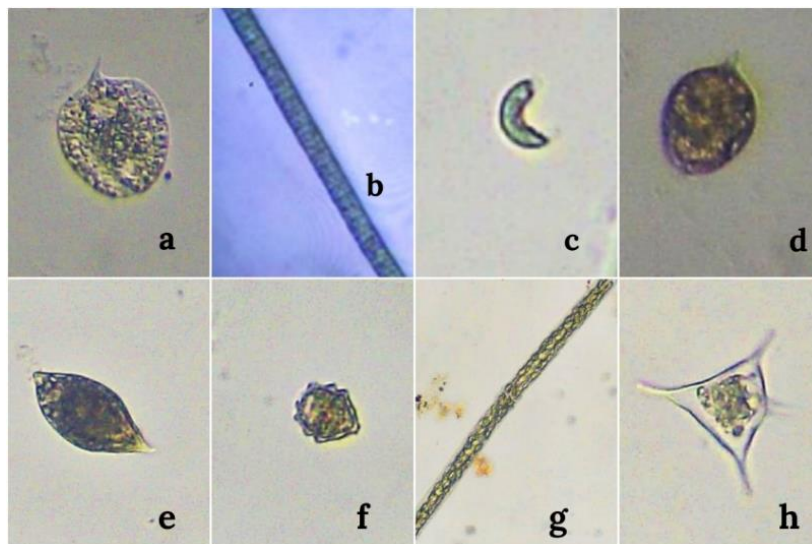


Fig. 23. a. *Phacus* sp., b. *Planktothrix* sp., c. *Monoraphidium* sp., d. *Lepocinclis pseudoovum*, e. *Euglena* sp., f. *Peridinium* sp., g. *Haplotaenium* sp., h. *Staurodesmus* sp.

Table 1. Frequency of phytoplankton enumerated per mL of concentrated sample after fixation with Lugol's Iodine in Carambolim I, Carambolim II, Batim I, Batim II

Taxonomic Group	Frequency of phytoplankton			
	Carambolim I	Carambolim II	Batim I	Batim II
<b>Bacillariophyta</b>				
<i>Aulacosiera</i>	8	71	0	0
<i>Cyclotella</i>	0	0	2	2
<i>Cymbella</i>	0	0	9	5
<i>Mastogloia</i>	17	0	8	6
<i>Melosira</i>	7	4	11	5
<i>Navicula</i>	68	45	33	19
<i>Nitzschia</i>	127	81	131	140
<i>Pinnularia</i>	29	21	4	11
<i>Synedra</i>	165	33	0	0
<b>Chlorophyta</b>				
<i>Ankistrodesmus</i>	52	11	3	18
<i>Closterium</i>	114	204	36	124
<i>Coelastrum</i>	10	80	21	36
<i>Comasiella</i>	0	0	0	16
<i>Cosmarium</i>	21	23	6	1
<i>Dimorphococcus</i>	27	20	32	19
<i>Haplotaenium</i>	4	8	4	4
<i>Kirchneriella</i>	33	44	32	16
<i>Micrasterias</i>	16	16	20	36
<i>Monoraphidinium</i>	90	52	20	60
<i>Pediastrum</i>	30	32	16	48
<i>Scenedesmus</i>	72	32	36	41
<i>Staurastrum</i>	72	80	64	92
<i>Staurodesmus</i>	6	23	0	0
<i>Tetrallantos lagerheimii</i>	25	16	8	14
<i>Xanthodinium eckertii</i>	0	0	0	10

<b>Dinophyta</b>				
<i>Dinophysis</i>	0	0	3	0
<i>Peridinium</i>	4	0	125	10
<b>Euglenophyta</b>				
<i>Euglena</i>	56	63	12	16
<i>Lepocinclis pseudoovum</i>	23	13	0	0
<i>Phacus</i>	50	19	47	22
<i>Trachelomonas</i>	28	16	78	28
<b>Cyanophyta</b>				
<i>Anabaena</i>	4	3	0	0
<i>Leptolyngbya</i>	0	0	2	6
<i>Merismopedia</i>	0	0	3	0
<i>Oscillatoria</i>	0	0	16	25
<i>Phormidium</i>	0	0	8	10
<i>Planktothrix</i>	11	3	4	0
<i>Pseudoanabaena</i>	27	22	6	8
<i>Syctonema</i>	16	11	0	0

Table 2. Diversity indices (Simpson and Shannon) for different sampling sites (Carambolim I, Carambolim II, Batim I, and Batim II)

<b>Diversity Index</b>	<b>Carambolim I</b>	<b>Carambolim II</b>	<b>Batim I</b>	<b>Batim II</b>
Simpson	0.9349	0.9234	0.9166	0.9191
Shannon	2.992	2.912	2.843	2.875

#### 4.4. Isolation, Culturing and Identification of Diatoms:

Four diatom isolates were obtained, one from each sample, which were identified with the aid of Tomas (1997) key. The isolates were identified to be *Nitzschia* sp., *Navicula* sp., *Cymbella* sp., and *Pinnularia* sp.



Fig. 24. *Nitzschia* sp. isolated from Carambolim I, observed under an inverted microscope at 400x magnification.



Fig. 25. *Navicula* sp. isolated from Carambolim II, observed under an inverted microscope at 400x magnification.

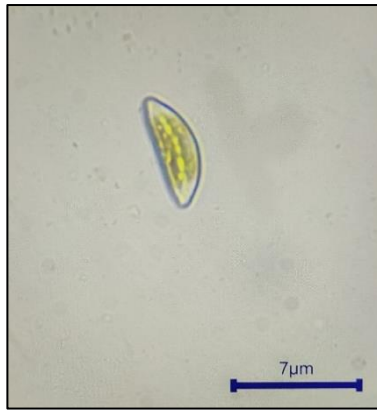


Fig. 26. *Cymbella* sp. isolated from Batim I, observed under an inverted microscope at 400x magnification.



Fig. 27. *Pinnularia* sp. isolated from Batim II, observed under an inverted microscope at 400x magnification.

The growth cycles of the isolated diatoms were assessed by regular enumeration using a hemocytometer.

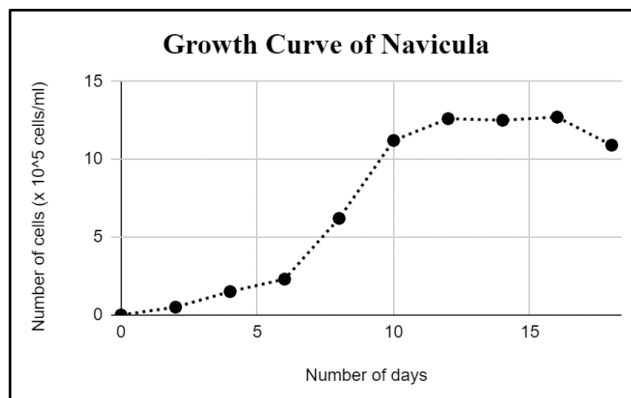


Fig. 28. A line graph depicting the growth curve of *Navicula* sp., enumerated using a hemocytometer and expressed as number of cells x 10<sup>5</sup> cells/mL.

*Navicula* sp. showed logarithmic growth from Day 6 to Day 10 of incubation, the cell count increasing from  $2.6 \times 10^5$  cells/mL to  $11.2 \times 10^5$  cells/mL, after which the increase in the cell density gradually slowed. The growth curve ends on Day 16 beyond which *Navicula* sp. showed a decline in the cell density.

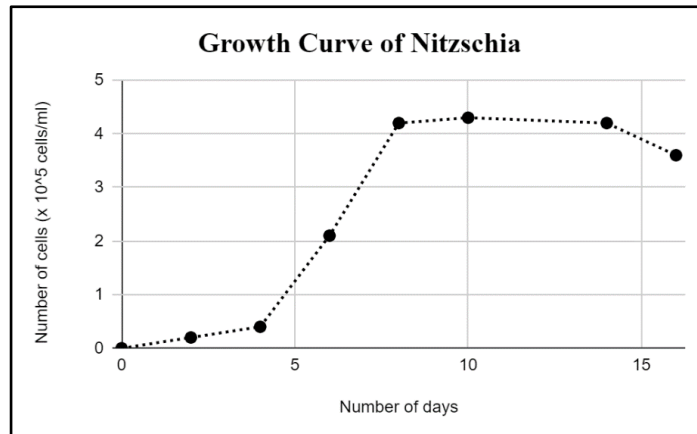


Fig. 29. A line graph depicting the growth curve of *Nitzschia* sp., enumerated using a hemocytometer and expressed as number of cells  $\times 10^5$  cells/mL.

*Nitzschia* sp. showed an increase in cell density from day 4 to day 8 of incubation with the number of cells rising from  $0.4 \times 10^5$  cells/mL to  $4.2 \times 10^5$  cells/mL, signifying the logarithmic phase. Thereafter, the cell density remained stable until day 14 after which the culture entered the death phase.

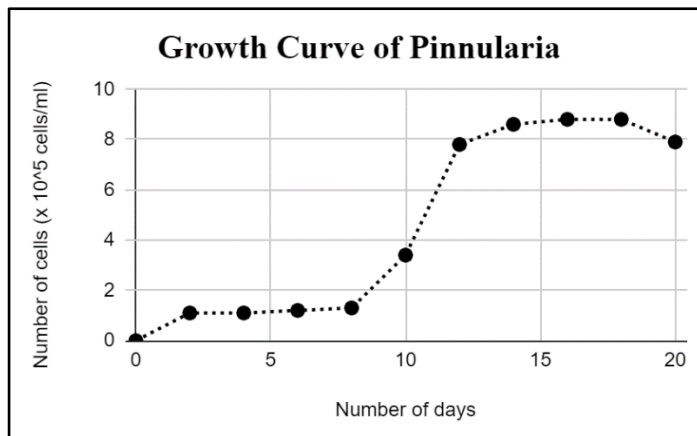


Fig. 30. A line graph depicting the growth curve of *Pinnularia* sp., enumerated using a hemocytometer and expressed as number of cells  $\times 10^5$  cells/mL.

The growth cycle of the isolated *Pinnularia* sp. was found to occur over a period of 22 days. The diatom cells entered the logarithmic phase on day 10 of incubation, the density increasing from  $3.4 \times 10^5$  cells/mL to  $7.8 \times 10^5$  cells/mL. A decline in the cell density was observed on day 20 of incubation, indicating the end of the stationary phase and beginning of the death phase.

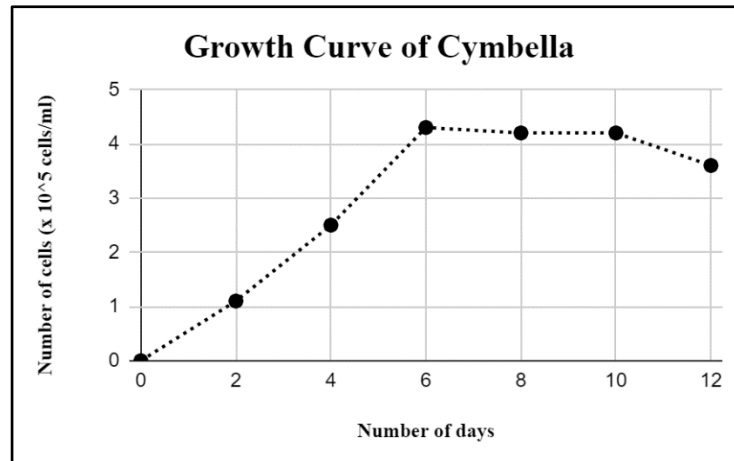


Fig. 31. A line graph depicting the growth curve of *Cymbella* sp., enumerated using a hemocytometer and expressed as number of cells  $\times 10^5$  cells/mL.

The cell density of *Cymbella* sp. was observed to increase for the first six days of incubation, after which it remained stable until day 10 of incubation. A decline in the growth of the culture after twelve days of incubation indicated the end of the cell division and subsequent beginning of the death phase.

#### **4.6. Determining the potential of the isolated diatoms as a delivery system:**

##### **4.6.1. Frustule Purification:**

The colour of the cell pellet obtained changed from brown/brownish-green to transparent/white after incubation with hydrogen peroxide and

concentrated HCl. The frustules were visualised using light microscopy and appeared clean, devoid of any organic material.



Fig. 32. Light microscopy image of *Navicula* frustules (left) and *Cymbella* frustule (right) after acid and hydrogen peroxide treatment, observed at 200x magnification.

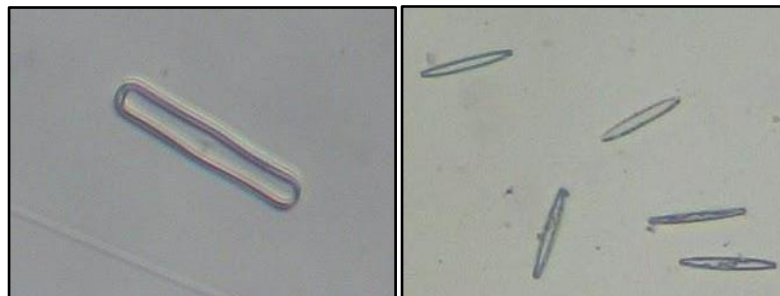


Fig. 33. Light microscopy image of *Pinnularia* frustule (left) and *Nitzschia* frustules (right) after acid and hydrogen peroxide treatment, observed at 200x magnification.

#### 4.6.2. Scanning Electron Microscopy (SEM) analysis:

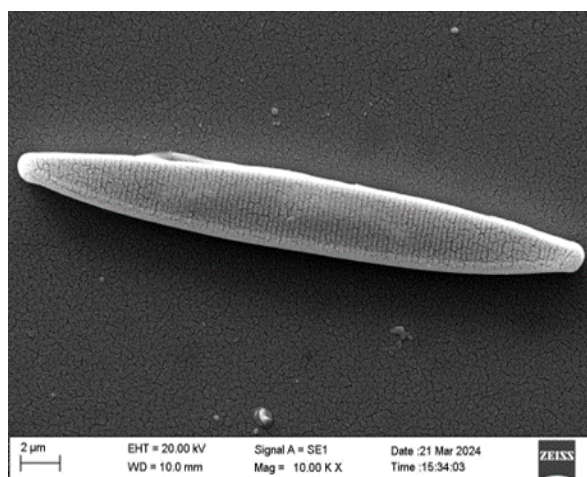


Fig. 34. SEM image of acid and hydrogen peroxide treated *Nitzschia* frustule.

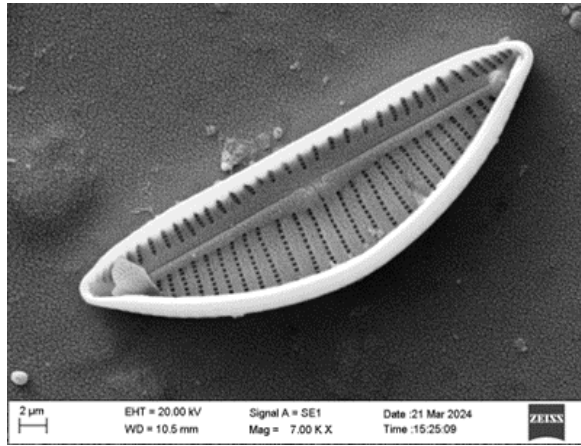


Fig. 35. SEM image of acid and hydrogen peroxide treated *Cymbella* frustule.

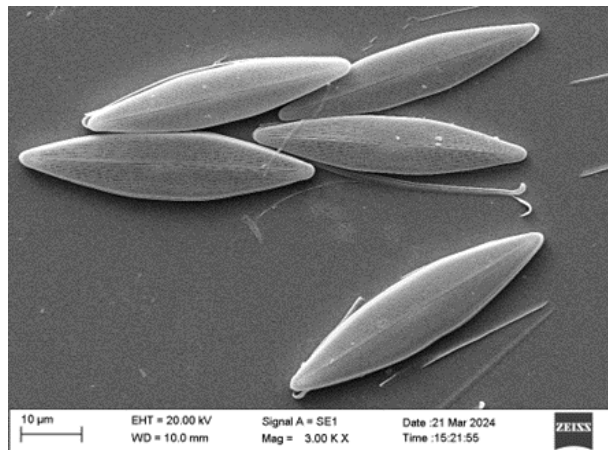


Fig. 36. SEM image of acid and hydrogen peroxide treated *Navicula* frustules.

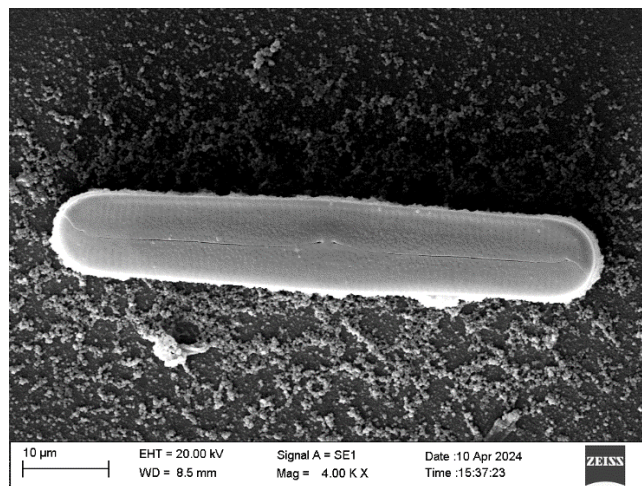


Fig. 37. SEM image of acid and hydrogen peroxide treated *Pinnularia* frustules.

Scanning electron microscopy revealed the mesoporous structure of the cleaned diatom frustules (Fig. 16, 17 and 18), the surfaces devoid of organic matter and ready for the process of functionalization.

#### 4.6.3. Surface Functionalization:

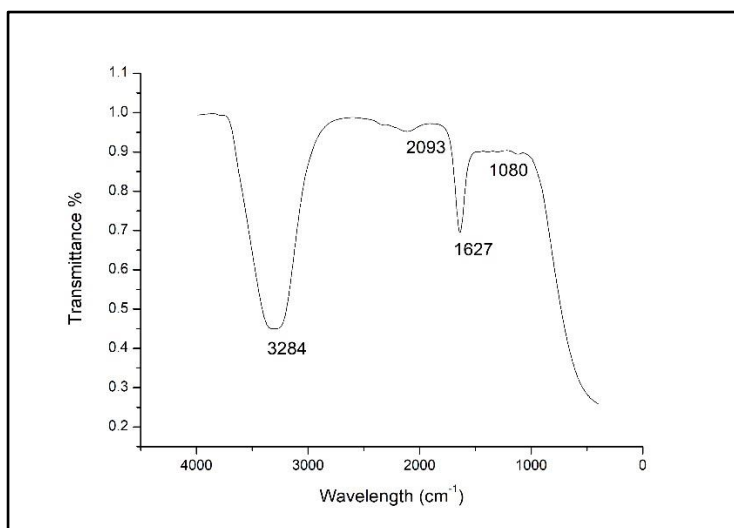


Fig. 38. FT-IR spectrum of *Cymbella* frustules after treating with APTES

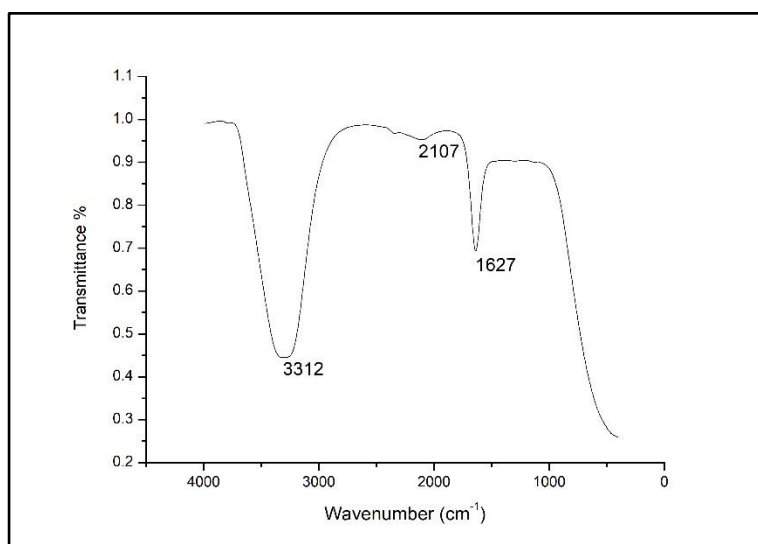


Fig. 39. FT-IR spectrum of *Pinnularia* frustules after treating with APTES

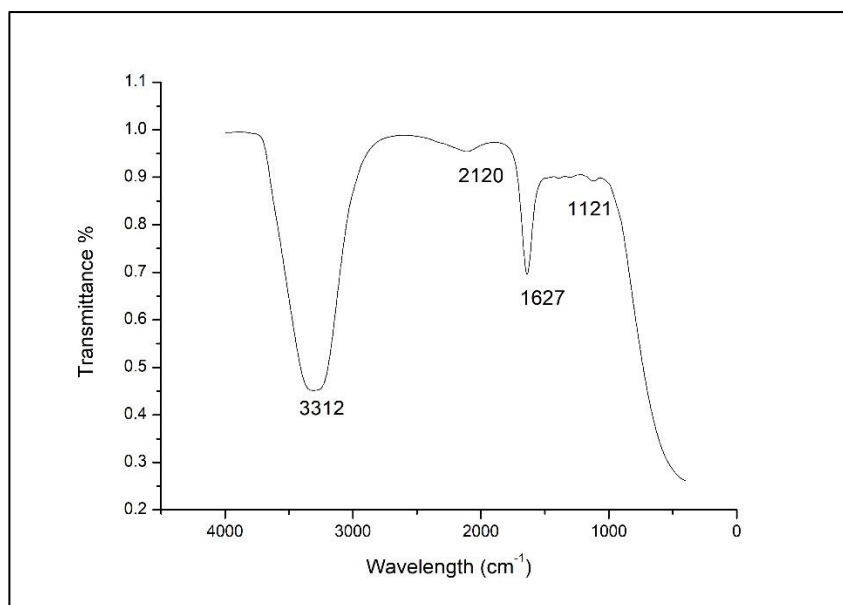


Fig. 40. FT-IR spectrum of *Nitzschia* frustules after treating with APTES

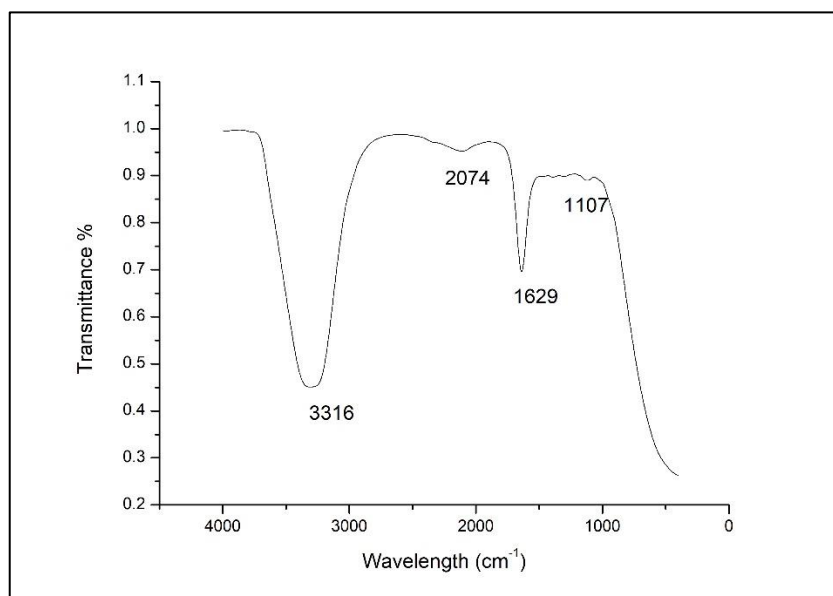


Fig. 41. FT-IR spectrum of *Navicula* frustules after treating with APTES

The FT-IR spectra of the frustules of each sample after treatment with the silanizing agent APTES are depicted in Fig. 38, 39, 40 and 41. The peaks visualised at  $1627\text{ cm}^{-1}$  (Fig. 38, 39, 40) and  $1629\text{ cm}^{-1}$  (Fig. 41) are due to the presence of hydroxyl groups, including the Si–OH on the diatom biosilica surface (Qi, Wang, & Cheng, 2016) respectively.

The peaks obtained at  $3284\text{ cm}^{-1}$ ,  $3312\text{ cm}^{-1}$ ,  $3316\text{ cm}^{-1}$ , can be attributed to hydrogen bonding, specifically N–H stretching, indicating that the addition of the amino group on the frustule has occurred, while the smaller peaks at  $1080\text{ cm}^{-1}$ ,  $1121\text{ cm}^{-1}$ ,  $1107\text{ cm}^{-1}$  are associated with Si-O-Si bonding in the frustule structure(Bayramoglu et al., 2013).

#### 4.6.4. Drug Loading:

The quantity of frustules utilised for loading of the drug was 10mg for each sample. Upon addition of the drug, the amount of drug loaded was determined by desorption in acetone, and determining the concentration of the drug using a standard calibration curve (Mancera-Andrade et al., 2019).

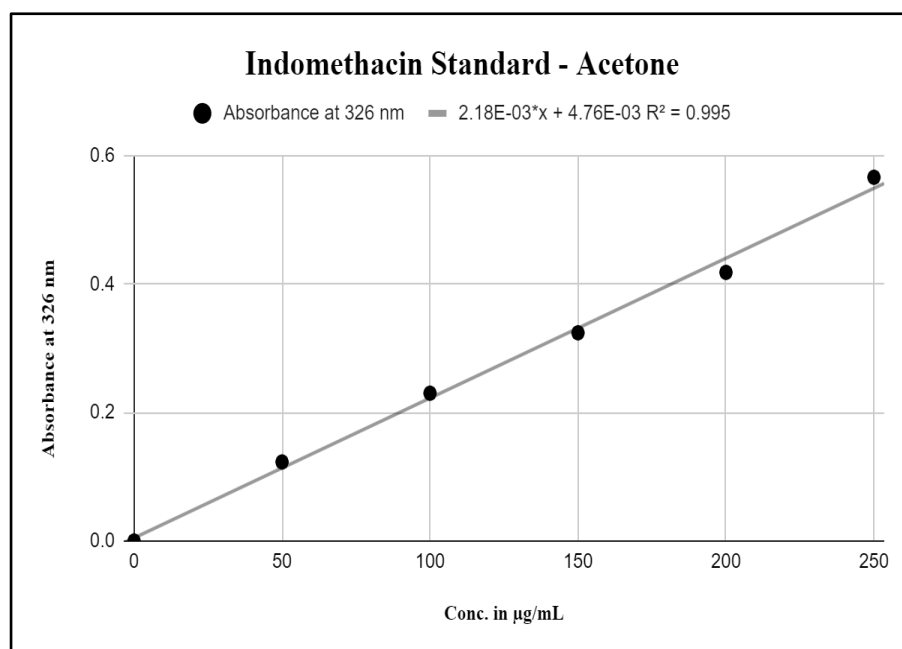


Fig. 42. A calibration curve for Indomethacin created using acetone as the solvent.

The loading capacity (LC) and encapsulation efficiency (EE) was evaluated for each sample. Table 3. shows the amount of drug loading and the corresponding LC and EE of the isolate determined by the following formulas (Aw et al., 2012):

<p><b><i>Drug loading capacity</i></b> = <i>weight of drug in frustules / weight of frustules</i></p> <p style="text-align: center;"><math>\times 100 \%</math></p> <p><b><i>Encapsulation efficiency</i></b> = <i>weight of drug in frustules / amount of drug added</i> <math>\times 100\%</math></p>
---

<b>Diatom culture</b>	<b>Amount of drug loaded</b>	<b>LC (%)</b>	<b>EE (%)</b>
<i>Nitzschia</i> sp..	0.88 mg	8.8	11
<i>Navicula</i> sp..	1.32 mg	13	16.5
<i>Cymbella</i> sp..	1.21 mg	12.1	15.1
<i>Pinnularia</i> sp..	2.63 mg	26.3	32.8

Table 3. The loading capacity and encapsulation efficiency observed for each sample.

Among the isolates tested for their potential use in a delivery system, *Pinnularia* sp. showed the best LC and EE %, the values being 26.3% and 32.8% respectively. *Navicula* sp. followed, exhibiting a LC of 13% and EE of 16.5%. *Cymbella* sp. demonstrated similar results with a 12.1 % LC and 15.1 % EE. *Nitzschia* sp. showed the least LC and EE values among the isolates, resulting in a loading capacity of 8.8% and efficiency for encapsulation to be 11%.

#### 4.6.5 In-vitro drug release:

*Nitzschia* frustules depicted a release pattern typically observed, an initial burst release followed by a sustained release period (Bariana et al., 2013 & Cicco et al., 2015). Rapid release of indomethacin occurred from the pores in the first hour (Fig. 43), accounting for 27.31% of the drug loaded. This increased to 45.45% towards the end of the second hour, and 91.67% of the loaded drug was released within the first three hours. The remaining drug was released in a sustained manner over the concluding 24 hours.

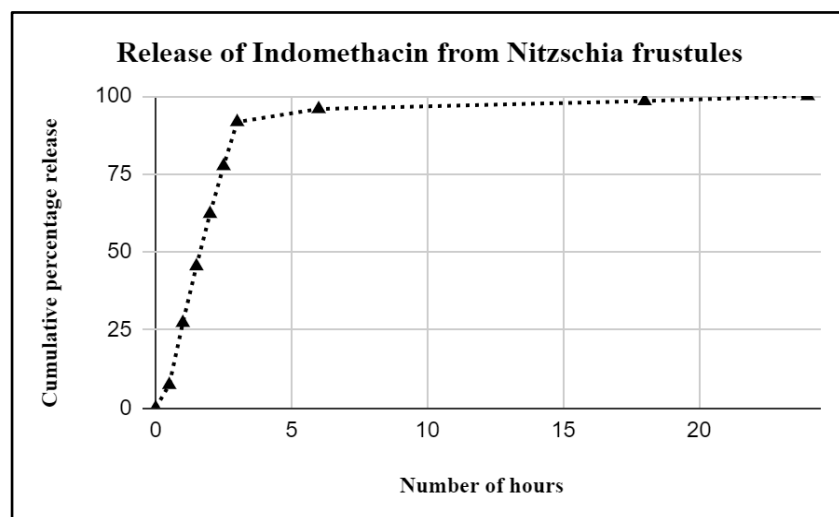


Fig. 43. Cumulative percentage release of indomethacin from *Nitzschia* frustules over a period 24 hours.

Indomethacin release from *Navicula* also showed an initial burst release of 80.77% in the first two hours. By the end of the first 18 hours, 89.27% of the drug release had occurred; the remaining percentage of drug release occurred in its entirety at the end of 48 hours of incubation (Fig. 44.).

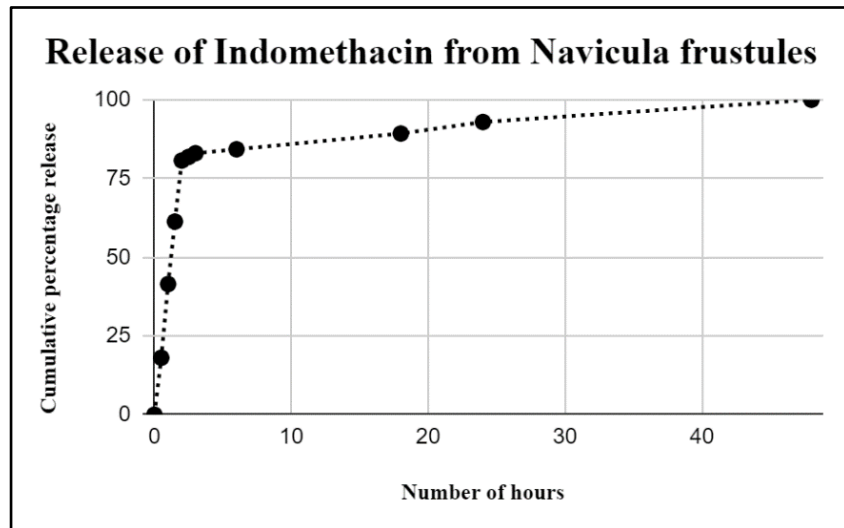


Fig. 44. Cumulative percentage release of indomethacin from *Navicula* frustules over a period 48 hours.

For *Cymbella*, the release of indomethacin occurred over a period of 72 hours, with the initial burst release occurring in the first three hours, accounting to 88% of the total loaded drug.

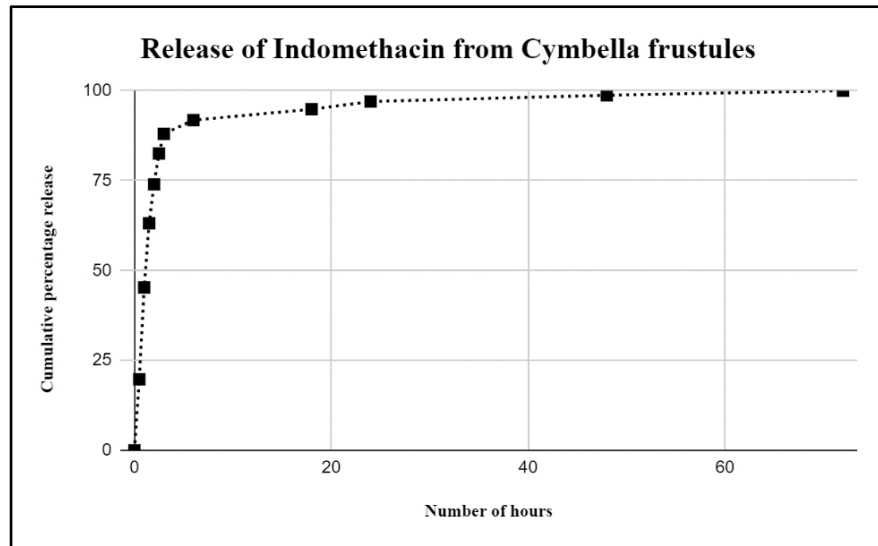


Fig. 45. Cumulative percentage release of indomethacin from *Cymbella* frustules over a period 72 hours.

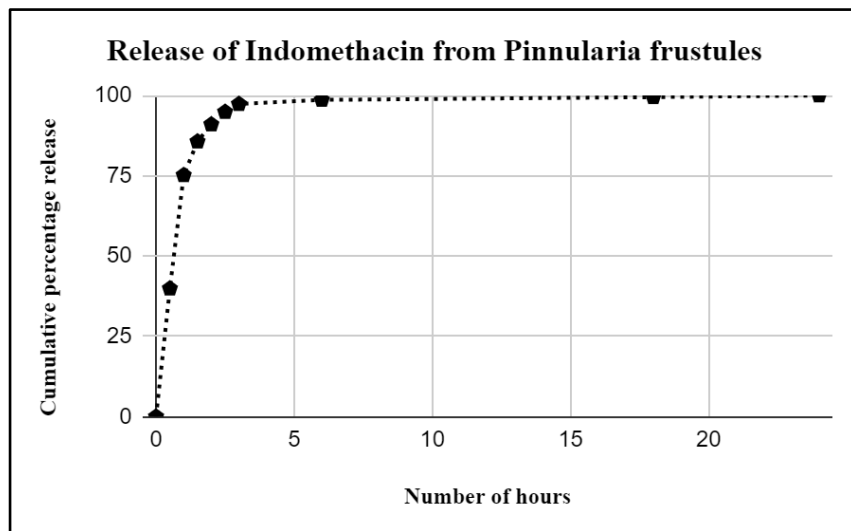


Fig. 46. Cumulative percentage release of indomethacin from *Pinnularia* frustules over a period 24 hours.

The release of Indomethacin from the loaded *Pinnularia* frustules (Fig. 46.) occurred in its entirety within the first 24 hours of incubation, depicting a burst release 75.17% by the end of the first hour.

## 4.7. Evaluating the ability of the isolated diatoms to treat agricultural wastewater:

### 4.7.1. Production of Simulated Wastewater:



Fig. 47. Fine powder of fertiliser granules used for producing simulated wastewater.



Fig. 48. Set of flasks of *Pinnularia* (top) and *Cymbella* (bottom) prepared for analysing the potential of diatoms for agricultural wastewater treatment.



Fig. 49. Set of flasks of *Navicula* prepared for analysing the potential of diatoms for agricultural wastewater treatment.

## 4.7.2. Analysis of nutrient composition:

### 4.7.2.1 Variation in Phosphate content:

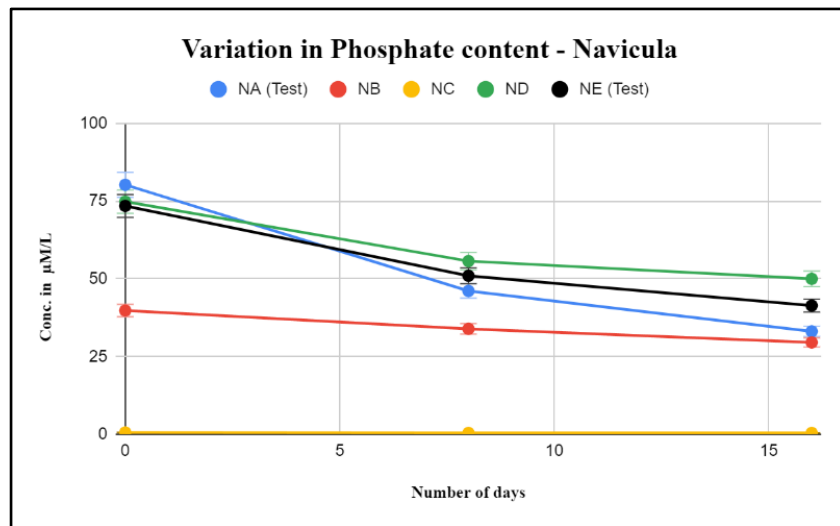


Fig. 50. A line graph showing variation in phosphate content in the simulated wastewater over the period of inoculation for the test and control flasks of *Navicula*.

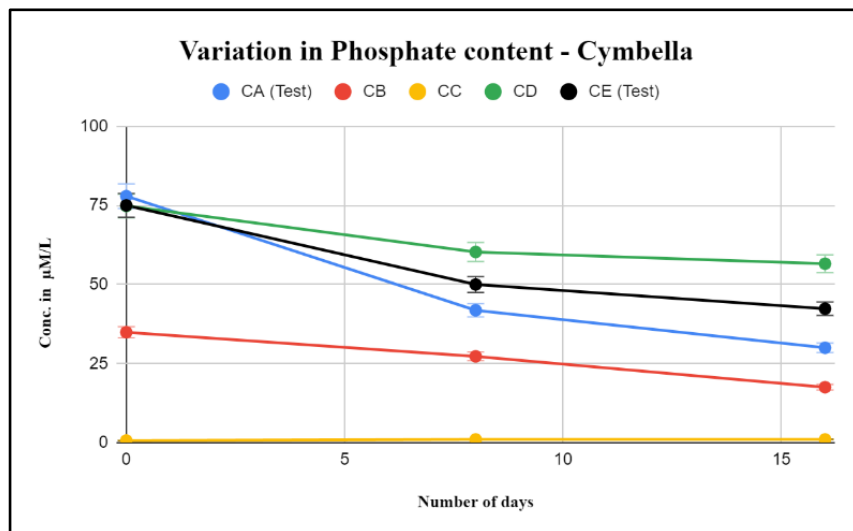


Fig. 51. A line graph showing variation in phosphate content in the simulated wastewater over the period of inoculation for the test and control flasks of *Cymbella*.

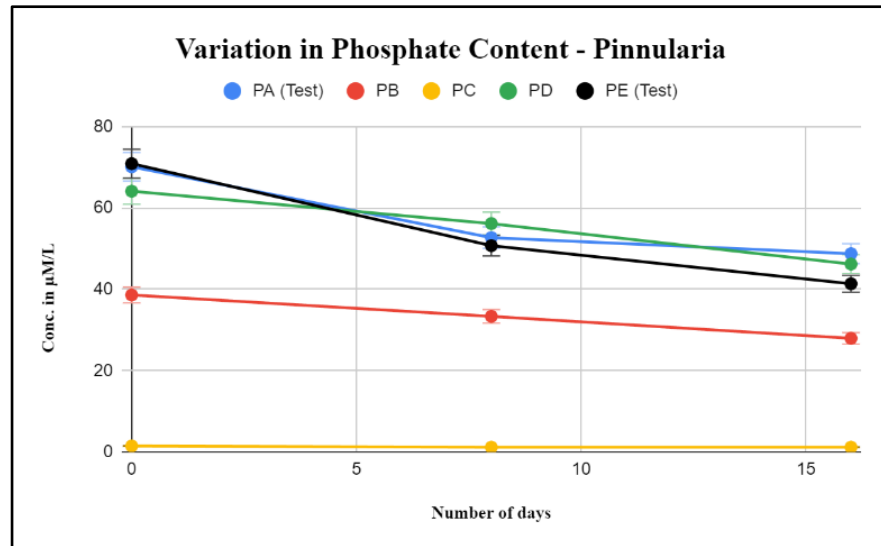


Fig. 52. A line graph showing variation in phosphate content in the simulated wastewater over the period of inoculation for the test and control flasks of *Pinnularia*.

The phosphate content in the flasks were evaluated on Day 0, Day 8 and Day 16 for test and control. Upon completion of the period of incubation, *Navicula* sp. caused a decline in the phosphate content in the NA flask (supplemented with f/2 components), reducing the initial concentration of 80.2 µM/L to a final concentration of 33.08 µM/L, showing a Relative percent reduction of 58.75% compared with the ND flask (control) which showed a reduction of 33.18%. The test flask without f/2 components (NE) caused a reduction of 43.63%.

For *Cymbella* sp., the concentration of phosphates in test flask supplemented with f/2 (CA) was reduced, depicting a relative percentage reduction compared with the CD control (24.41%) of 61.51% while the test flask without supplementation of f/2 depicted a decrease in phosphate concentration of 43.55%. However, *Pinnularia* sp.. could show a relative reduction of only 30.47% in test flask PA & 28.33% in test flask PE, while

the control flask exhibited a reduction of 23.9% in the phosphate concentration.

The analysis of variance (ANOVA) conducted on phosphate content across various flasks, for *Navicula* sp., yielded statistically significant differences ( $F_{(3, 8)} = 8.64, p = 0.0068$ ). Similarly, for *Cymbella* sp., ANOVA revealed a significant difference in phosphate content between test and control flasks ( $F_{(3, 8)} = 8.50, p = 0.0072$ ). Furthermore, focusing on different groups (PA, PB, PC, and PD) for *Pinnularia* sp., the single-factor ANOVA demonstrated statistically significant differences in phosphate content among the groups ( $F_{(3, 8)} = 34.26, p < 0.0001$ ).

#### **.4.7.2.2. Variation in Ammonia content:**



Fig. 53. Test tubes depicting a series of standards of Ammonia prepared with Ammonium chloride.

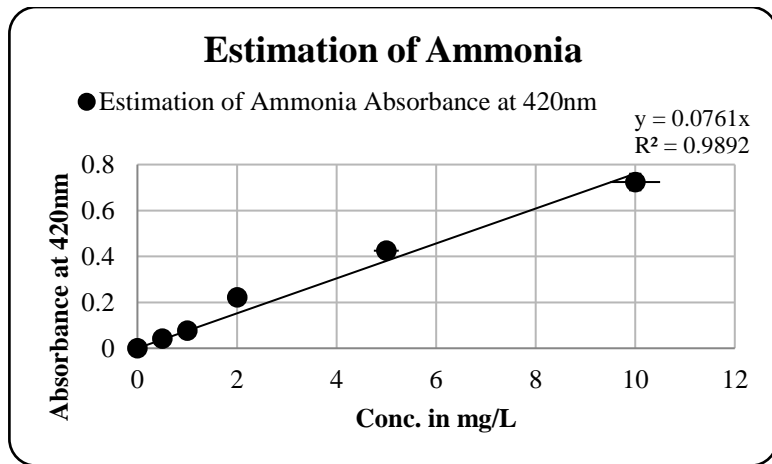


Fig. 54. A graph depicting the calibration curve prepared for estimation of ammonia.

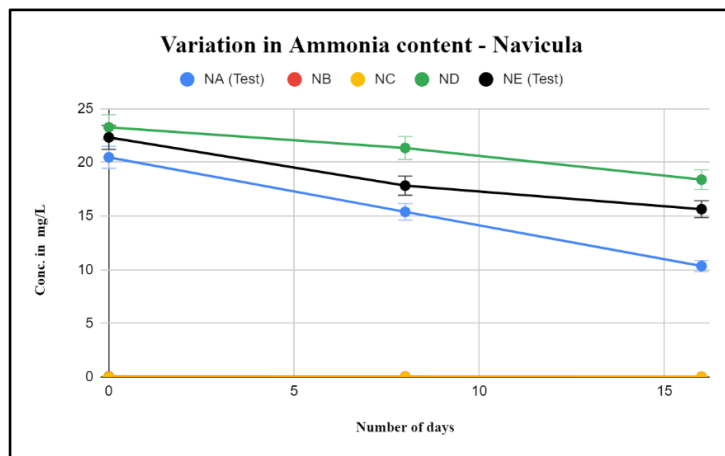


Fig. 55. A line graph showing variation in ammonia content in the simulated wastewater over the period of inoculation for the test and control flasks of *Navicula*.

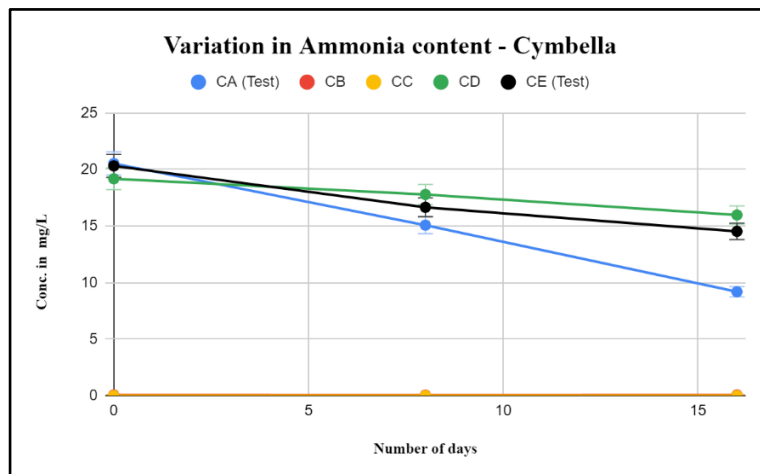


Fig. 56. A line graph showing variation in ammonia content in the simulated wastewater over the period of inoculation for the test and control flasks of *Cymbella*.

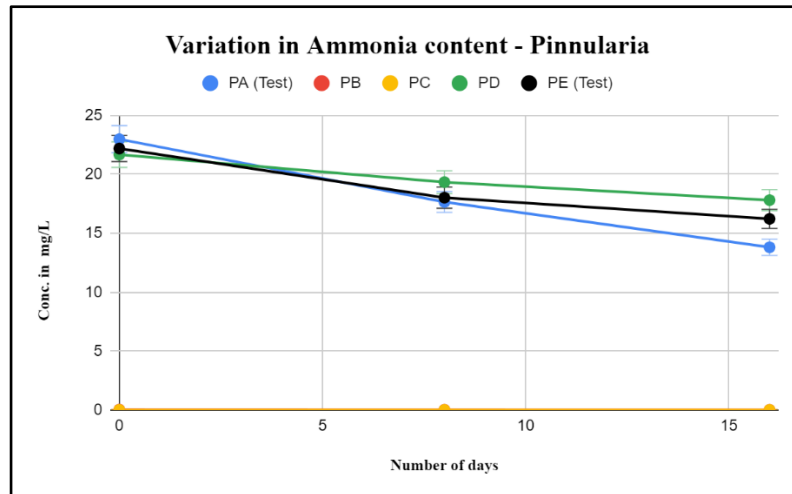


Fig. 57. A line graph showing variation in ammonia content in the simulated wastewater over the period of inoculation for the test and control flasks of *Pinnularia*.

The ammonia content in the flasks was assessed on Day 0, Day 8, and Day 16 for both test and control groups. Following the incubation period, *Navicula* sp.. displayed a Relative percent reduction of 49.48% in test flask NA surpassing the control's reduction of 20.97%, while a reduction of 29.64% was observed in the NE test flask. Conversely, *Cymbella* sp. illustrated a relative percentage reduction of 55.2% in the CA test flask compared to the control's reduction of 16.68% (CD). Although the CE test flask showed reduction in the ammonia content of 28.49%. *Pinnularia* sp. exhibited a relative reduction of only 39.9% in the PA test flask and 26.95% in the PE test flask, contrasting with the control flask's reduction of 17.8% in ammonia concentration.

The analysis of variance demonstrated significant differences in ammonia content reduction between test and control flasks across all three isolates tested, with a significance level of  $p < 0.05$ . For *Navicula* sp., ANOVA

indicated a highly significant difference among groups ( $F(3, 8) = 43.72, p < 0.0001$ ). Similarly, significant differences were observed among groups for *Cymbella* sp.. ( $F(3, 8) = 21.11, p = 0.00037$ ) and *Pinnularia* sp.. ( $F(3, 8) = 58.49, p < 0.00001$ ).

#### 4.7.2.3. Variation in Nitrite content:

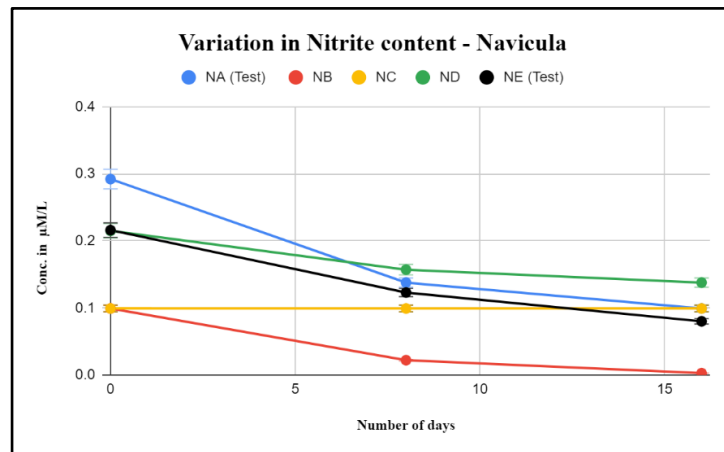


Fig. 58. A line graph showing variation in nitrite content in the simulated wastewater over the period of inoculation for the test and control flasks of *Navicula*.

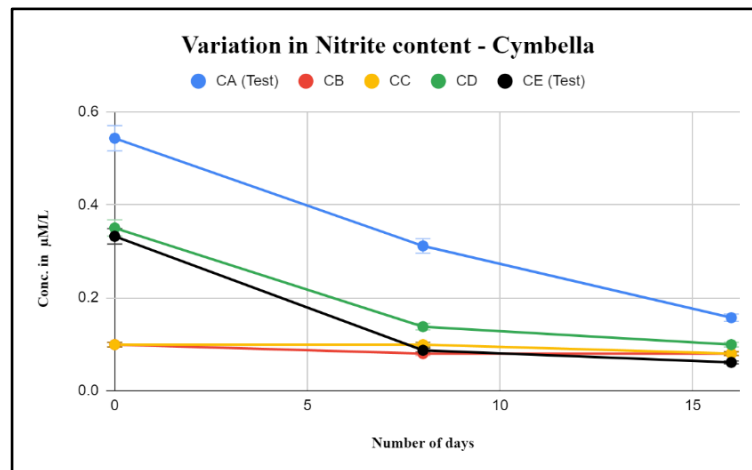


Fig. 59. A line graph showing variation in nitrite content in the simulated wastewater over the period of inoculation for the test and control flasks of *Cymbella*.

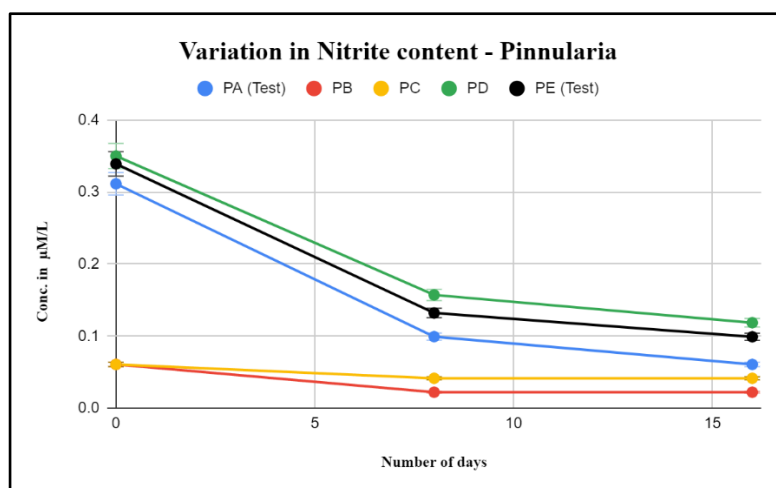


Fig. 60. A line graph showing variation in nitrite content in the simulated wastewater over the period of inoculation for the test and control flasks of *Pinnularia*.

The nitrite content within the flasks was evaluated at three intervals: Day 0, Day 8, and Day 16, for both the test and control groups. After the incubation period, *Navicula* sp.. exhibited a relative percent reduction of 65.8% in NA test flask, and 62.96% in NE test flask, slightly surpassing the control's reduction of 61.5%. Conversely, *Cymbella* sp.. demonstrated a relative reduction of 72.2% (CA test flask), and 81.62% in the CE test flask, showing relatively higher reductions compared to the control's reduction of 70.8%. *Pinnularia* sp.. showcased in the PA test flask a notable reduction of 80.6%; 70.79% in PE test flask, notably higher than the control flask's reduction of 67.6% in nitrite concentration.

The ANOVA results indicate that there is no statistically significant difference among the groups ( $F(3, 8) = 3.36$ ,  $p = 0.0759$ ), with a between-groups variance of 0.037 for *Navicula* sp. Similarly, for *Cymbella* sp. no statistically significant difference among the test and control flasks was observed for reduction of nitrite content ( $F(3, 8) = 2.94$ ,  $p = 0.09896$ ). The

ANOVA results also revealed that there is no statistically significant difference among the control and the test flasks ( $F(3, 8) = 2.50, p = 0.133$ ).

#### 4.7.2.4. Variation in Nitrate Content:

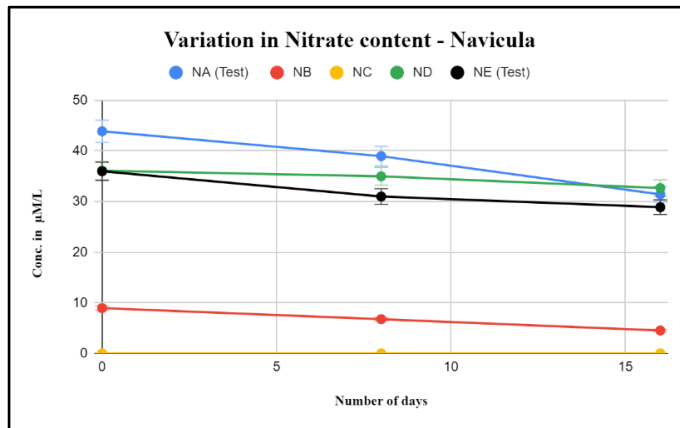


Fig. 61. A line graph showing variation in nitrate content in the simulated wastewater over the period of inoculation for the test and control flasks of *Navicula*.

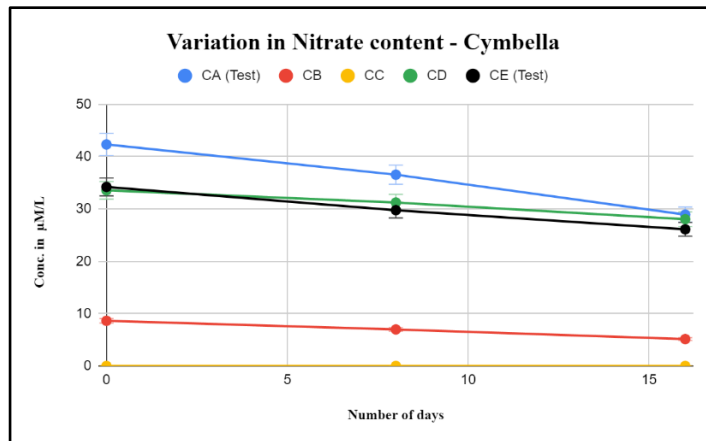


Fig. 62. A line graph showing variation in nitrate content in the simulated wastewater over the period of inoculation for the test and control flasks of *Cymbella*.

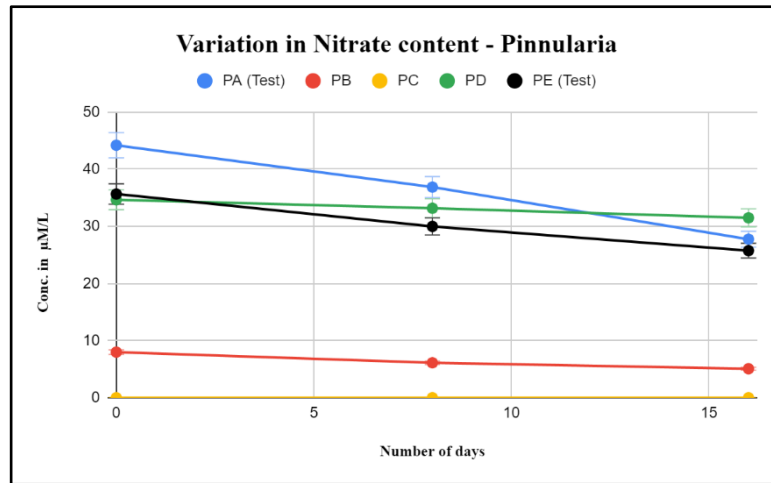


Fig. 63. A line graph showing variation in nitrate content in the simulated wastewater over the period of inoculation for the test and control flasks of *Pinnularia*

The nitrate content within the flasks was assessed at three intervals: Day 0, Day 8, and Day 16, for both the test and control groups. Following the incubation period, *Navicula* sp. in the NA test flask displayed a relative percent reduction of 28.3%, which exceeded the control's reduction of 9.5% and the NE test flask's reduction of 19.73%. Similarly, *Cymbella* sp. showed a relative reduction of 31.6% in the CA test flask and 23.67% in the CE test flask, slightly higher than the control's reduction of 16.4%. Notably, *Pinnularia* sp. exhibited a substantial reduction of 37.2% in the PA test flask and 27.79% in the PE test flask, significantly higher than the control flask's reduction of 9.1% in nitrate concentration.

The statistical analysis using one-factor ANOVA indicated a highly significant difference for reduction of nitrate content among the test and control flasks for *Navicula* sp. ( $F(3, 8) = 94.31, p < 0.0001$ ). Also, for *Cymbella* sp., the results indicated a highly significant difference among the groups ( $F(3, 8) = 66.82, p < 0.00001$ ). A significant difference for reduction

of nitrate content among the test and control flasks was also noted for *Pinnularia* sp., ( $F(3, 8) = 56.09, p < 0.00001$ ).

#### 4.7.3. Determination of cell density:

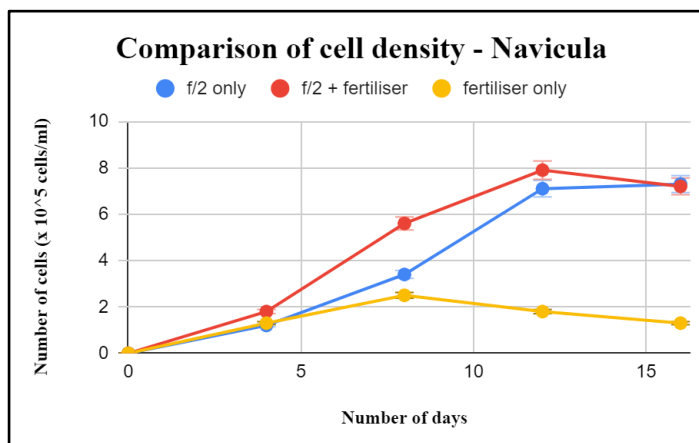


Fig. 64. A line graph showing the comparison of cell density of *Navicula* between the flask control flask, containing just f/2 medium and the culture, and the test flask containing f/2 supplemented simulated wastewater & plainly wastewater without f/2, over a 16-day incubation period.

In comparison with the control flask containing f/2 medium inoculated with the isolate *Navicula* sp., the test flask showed a similar pattern for increase in the cell density, although the increase from the initial concentration was found to vary from  $3.4 \times 10^5$  cells/mL for the control flask to  $5.6 \times 10^5$  cells/mL for the test flask with f/2 and  $2.5 \times 10^5$  cells/mL for test flask without f/2 on day 8 of incubation. The final cell density in the control flask was calculated to be  $7.3 \times 10^5$  cells/mL and f/2 supplemented test flask was determined to be  $7.2 \times 10^5$  cells/mL on day 16, and  $1.3 \times 10^5$  cells/mL for test flask without f/2 components.

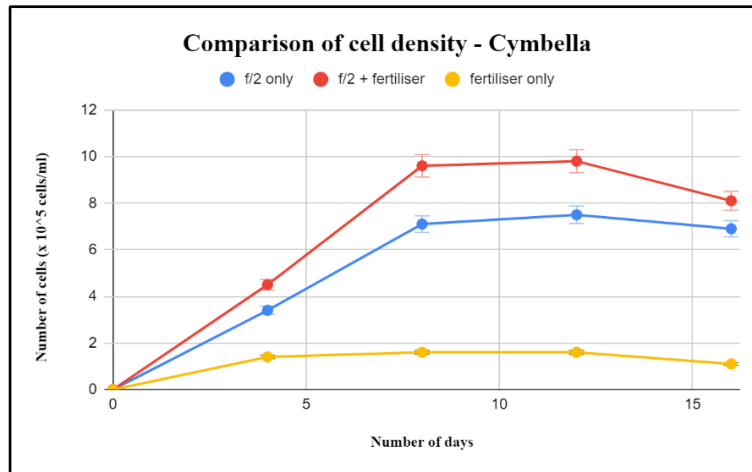


Fig. 65. A line graph showing the comparison of cell density of *Cymbella* between the flask control flask, containing just f/2 medium and the culture, and the test flask containing f/2 supplemented simulated wastewater & plainly wastewater without f/2, over a 16-day incubation period.

Similar observations were made for *Cymbella* sp., with the final cell densities accounting to  $6.9 \times 10^5$  cells/mL in the control flask and  $8.1 \times 10^5$  cells/mL in the CA test flask (containing simulated wastewater supplemented with f/2) and  $1.1 \times 10^5$  cells/mL in the CE test flask containing no f/2 components.

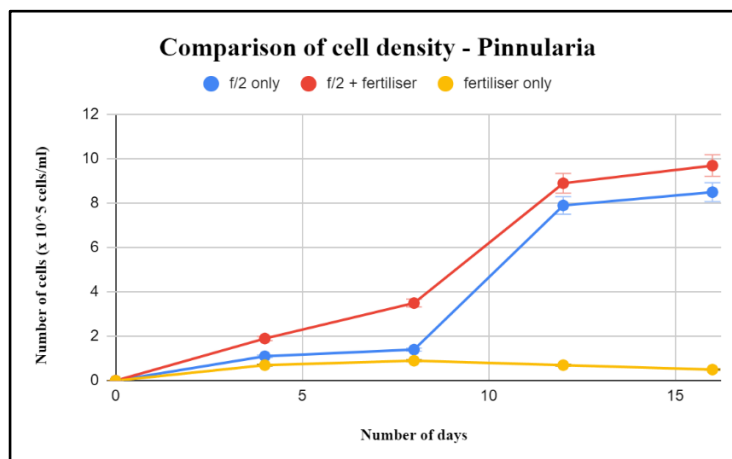


Fig. 66. A line graph showing the comparison of cell density of *Pinnularia* between the flask control flask, containing just f/2 medium and the culture, and the test flasks containing f/2 supplemented simulated wastewater & plainly wastewater without f/2, over a 16-day incubation period.

For *Pinnularia* sp., the cell density at the end of the incubation period was found to be  $8.5 \times 10^5$  cells/mL and  $9.7 \times 10^5$  cells/mL and  $0.5 \times 10^5$  cells/mL for the control and PA test flask and PE test flask, respectively.

## **DISCUSSION**

Measuring dissolved oxygen is crucial in studying aquatic environments, offering key insights into biological and biochemical processes. It's a vital factor for aquatic life and indicates the water's ability to regulate organic matter (Wetzel & Likens, 2000). The levels of dissolved oxygen primarily rely on the balance between photosynthetic oxygen production and overall plankton respiration (Denny, Cren, & Lowe-McConnell, 1981). DO levels below 1 mg/L are considered hypoxic, while DO levels greater than 6.5mg/L symbolise healthy aquatic environments (Environmental Protection Agency, 2012). Thus, Batim and Carambolim lake, with DO values greater than 6.5 mg/L are confirmed as healthy lakes, capable of supporting aquatic flora and fauna.

The primary source of silica is typically the weathering of natural rock formations, resulting in higher concentrations of silica in freshwater environments (Nasser, 2013). As noted by Schindler (1978) silica serves as an additional factor constraining the growth of diatoms. Only a slight increase in silicate levels were observed between the consecutive samplings in Batim lake. As per literature, the increase in silicate content from September 2023 to October 2023 in Carambolim lake could be attributed to rainfall, which favours the dissolution of silica in the water (Atkins, 1926).

Jeppesen et al. (1997) suggested that phosphate concentrations ranging from 0.5  $\mu\text{M/L}$  to 1.0  $\mu\text{M/L}$  serve as the threshold indicating its significance as a nutrient in natural water bodies. The concentration of phosphates is higher

than this threshold value for Carambolim II & Batim I, being 1.16  $\mu\text{M/L}$  & 1.7  $\mu\text{M/L}$ , respectively. This anomaly could be attributed to anthropogenic influence (Ryland, 1994), or due to surface runoff during rain (Jeppesen et al. 1997).

In the majority of instances, nitrite is produced through the reduction of nitrate, although there are exceptions in certain lakes where it is thought to originate from the oxidation of ammonia, as discussed by Ketchum & Hutchinson in 1957. Normal values for nitrite in lakes fall in the range of 2-10  $\mu\text{g/L NO}_2\text{-N}$  (0.14  $\mu\text{M/L}$  – 0.7  $\mu\text{M/L}$  of nitrite). The low value for nitrite in Carambolim I is likely due to dilution of the lakewater due to rainfall as elucidated by Eddy & Williams (1987).

The diversity analysis showed Chlorophyta to be the dominant phylum in both of the samples collected from Carambolim Lake and Batim Lake. Some notable genera found in the investigated lakes are: *Scenedesmus*, *Pediastrum*, *Closterium*, *Cosmarium* & *Staurodesmus*. Some of the major diatoms belonged to the genera *Navicula*, *Nitzschia*, *Synedra* & *Aulacosiera*. Rodrigues & Sawaiker (2016) reported the phytoplankton diversity of some freshwater lakes in Goa, noting presence of genera belonging to Chlorophyta, such as *Scenedesmus* & *Pediastrum*.

Shannon's Diversity Index is a quantitative measure used in ecology to assess the diversity of species within a given community or ecosystem which takes into account both the richness (number of different species) and evenness

(relative abundance of each species) of species present in the community (Hd. & Odum, 1974). After analyzing the diversity within polluted and unpolluted ecosystems, Wilhm and Dorric (1968) determined that index values exceeding 3 indicate clean water & high diversity; values ranging from 1 to 3 signify moderate pollution & intermediate diversity, while those below 1 denote heavy pollution & low diversity. Applying this understanding to our study, the Shannon Diversity Index values for the samples, Carambolim I, Carambolim II, Batim I, and Batim II, fall within the range associated with moderate pollution & intermediate diversity. The Simpson diversity index is another measure of biodiversity or species diversity within a community. Unlike the Shannon diversity index, which takes into account both species richness and evenness, the Simpson index primarily focuses on the dominance or the probability that two randomly selected individuals in a community belong to the same species (Hd. & Odum, 1974). The values for Simpson index were recorded as 0.9349 for Carambolim I, 0.9234 for Carambolim II, 0.9166 for Batim I and 0.9191 for Batim II. These values indicate that the species are evenly distributed in the sampling site as elucidated by Tripathi et al., (2008).

In this investigation, the examination of isolates revealed that *Pinnularia* sp. exhibited the highest loading capacity (LC) at 26.3%, coupled with an associated loading efficiency (EE) of 32.8%. These findings resonate with previous studies, particularly those by Balas, Manzano, Horcajada, and Vallet-Regí (2006), who noted similar values in synthetic mesoporous silica ISBA-3. Kumeria et al. (2013) previously reported a notably high loading

capacity of 28.5%, achieving an impressive loading efficiency of 95% using frustules purified from diatomaceous earth. Comparatively, Bariana et al. (2013) observed loading capacities ranging from 14% to 24% for indomethacin in diatoms functionalized through phosphonic acids and silanes, indicating a range of efficacies depending on functionalization methods. Similarly, Mancera-Andrade et al. (2019) documented an EE of 17.92% for the drug isorhamnetin when utilizing purified frustules of diatom *Cyclotella*. Noteworthy is the study by Gnanamoorthy, Anandhan, and Prabu (2014), which reported a remarkable loading capacity of 33.33% for the drug streptomycin sulphate, indicating the potential for significant variations in loading capacity depending on the specific drug and carrier system utilized.

The in-vitro release study exhibited classic two-phase release kinetics: an initial burst followed by sustained release, consistent with literature findings. Complete drug release occurred within 24-72 hours for the tested diatom isolates. The initial burst phase is attributed to drug release from the outer surface of the frustules, while sustained release is due to drug release from the inner pores of the frustule structure (Maher, Kumeria, Aw, & Losic, 2018).

For the use of the isolates in treatment of agricultural wastewater, reduction in the nutrient concentration present in the simulated wastewater, among the test and control flasks was found to be statistically significant for nitrate, phosphate and ammonia. For nitrite, the difference in the reduction among the test and the control flasks was determined to be statistically insignificant

at significance level  $p < 0.05$ . This could be attributed to the very low nitrite content present initially in the simulated wastewater, existing at the concentration of only 0.3 to 0.5  $\mu\text{M/L}$  in the test and control flask. Additionally, as mentioned earlier, nitrite in itself usually exists as an intermediate in ammonia assimilation (Ketchum & Hutchinson, 1957).

The test flasks with f/2 supplementation showed a significant reduction in nutrient concentrations compared to the uninoculated simulated wastewater control. However, a lower decrease was observed in flasks without f/2 supplementation. This disparity was attributed to the silicate concentration disparity: 3.64  $\mu\text{M/L}$  in the simulated wastewater versus 114.5  $\mu\text{M/L}$  in the f/2 supplemented flask. This discrepancy explains the lower cell density observed (as mentioned in section 4.7.3.) in the un-supplemented flasks, as silica serves as a limiting factor in diatom growth (Martin-Jézéquel, Hildebrand, & Brzezinski, 2000).

The decrease in the concentration of nutrients in the uninoculated control flask containing simulated wastewater is likely due to precipitation of phosphates by metals present within the wastewater leading to removal of free phosphate from the solution and a decrease in measured concentration (Spivakov, Maryutina, & Muntau, 1999). Ammonia reduction in the control flask can be attributed to abiotic volatilization of the ammonium present in the flask at an inclined pH, thus reducing free ammonia measured in the solution (Quinn, Asher, & Charlson, 1992). Nitrates present in the flask may be utilised by residual bacteria present within the flask, which by the proves

of biological denitrification could convert it to N<sub>2</sub> gas, thereby decreasing the measured value in solution.

*Navicula* sp. and *Pinnularia* sp. showed effective reduction in the nitrate concentration compared with the control flasks, 28.3% and 37.2% for the test flasks (supplemented with f/2), respectively, while the reduction in the control flasks was deduced to be 9.1% and 9.5%, respectively. *Navicula* sp. also depicted the best relative percent reduction for phosphate content when f/2 was supplemented in the simulated wastewater (58.75%). In comparison with other isolates and their respective controls, *Cymbella* sp. demonstrates the superior performance in reducing ammonia content. While *Navicula* sp. achieves a significant reduction with a relative percent reduction of 49.48% compared to its control's reduction of 20.97%, *Cymbella* sp. achieves an even higher reduction of 55.2% compared to its control's reduction of 16.68% when supplemented with f/2. A diatom consortium comprising of *Navicula* sp. & *Cymbella* sp. among others has previously shown to cause reduction in nutrient content of 95.1% for nitrogen and 88.9% for phosphorus (Marella, Parine, & Tiwari, 2018).

## CONCLUSION

This study evaluated the physico-chemical parameters of the sampling sites alongside isolation of four diatoms from the selected wetlands, Carambolim Lake and Batim Lake. The isolates were identified to be *Nitzschia* sp., *Navicula* sp., *Cymbella* sp., and *Pinnularia* sp. The diversity study showed Chlorophyta (green algae) to be the dominant group among the phytoplankton observed across all samples. The findings of this study highlight the significance of the isolated diatoms in the field of drug delivery. Although *Nitzschia* sp. depicted a low loading capacity and encapsulation efficiency for the model drug Indomethacin, *Navicula* sp., *Pinnularia* sp. and *Cymbella* sp. showed comparable values to those reported in literature. While *Cymbella* sp. exhibited a more favorable, sustained release over 72 hrs, a higher loading capacity was observed in *Pinnularia* frustules (26.3%). The isolates tested for their ability to reduce nutrient concentration in a simulated wastewater showed significant results when supplemented with silica (in the form of f/2), with *Navicula* sp. emerging as the best candidate, being able to reduce phosphate content by 58.75%, ammonia content by 49.48% and nitrate content by 28.3%, comparable to those noted in literature. This study thus highlighted the significance of the freshwater diatom isolates in the fields of drug delivery and agricultural wastewater treatment.

## **FUTURE PROSPECTS**

- Optimisation of growth rate of the isolates in different growth media.
- Energy-dispersive X-ray (EDX) analysis of frustules before and after functionalisation for characterising their elemental composition.
- Brunauer-Emmett-Teller analysis to determine the specific surface area of the frustules.
- Optimisation of silanizing/surface functionalizing agent for enhancing loading capacity of the frustules.
- Monitoring drug release at different pH and their effect on the integrity of frustules.
- Extraction of valuable products from diatom culture cultivated in wastewater system & nutrient recycling.

## REFERENCES

1. Abou-Shanab, R. A. I., Ji, M.-K., Kim, H.-C., Paeng, K.-J., & Jeon, B.-H. (2013). Microalgal species growing on piggery wastewater as a valuable candidate for nutrient removal and biodiesel production. *Journal of Environmental Management*, 115, 257–264. doi:10.1016/j.jenvman.2012.11.022
2. Amano, Y., Takahashi, K., & Machida, M. (2011). Competition between the cyanobacterium *Microcystis aeruginosa* and the diatom *Cyclotella* sp. under nitrogen-limited condition caused by dilution in Eutrophic Lake. *Journal of Applied Phycology*, 24(4), 965–971. doi:10.1007/s10811-011-9718-8
3. Arumugham, S., Joseph, S. J., P M, G., Nooruddin, T., & Subramani, N. (2023). Diversity and ecology of freshwater diatoms as pollution indicators from the freshwater ponds of Kanyakumari District, Tamilnadu. *Energy Nexus*, 9, 100164. doi:10.1016/j.nexus.2022.100164
4. Ashekuzzaman, S. M., Forrestal, P., Richards, K., & Fenton, O. (2019). Dairy industry derived wastewater treatment sludge: Generation, type and characterization of nutrients and metals for agricultural reuse. *Journal of Cleaner Production*, 230, 1266–1275. doi:10.1016/j.jclepro.2019.05.025
5. Aslan, S., & Kapdan, I. K. (2006). Batch kinetics of nitrogen and phosphorus removal from synthetic wastewater by algae. *Ecological Engineering*, 28(1), 64–70. doi:10.1016/j.ecoleng.2006.04.003
6. Atkins, W. R. (1926). Seasonal changes in the silica content of natural waters in relation to the phytoplankton. *Journal of the Marine Biological*

- Association of the United Kingdom*, 14(1), 89–99.  
doi:10.1017/s0025315400007153
7. Aw, M. S., Bariana, M., Yu, Y., Addai-Mensah, J., & Losic, D. (2012). Surface-functionalized diatom microcapsules for drug delivery of water-insoluble drugs. *Journal of Biomaterials Applications*, 28(2), 163–174.  
doi:10.1177/0885328212441846
  8. Aw, M. S., Simovic, S., Yu, Y., Addai-Mensah, J., & Losic, D. (2012). Porous silica microshells from diatoms as biocarrier for drug delivery applications. *Powder Technology*, 223, 52–58.  
doi:10.1016/j.powtec.2011.04.023
  9. Balas, F., Manzano, M., Horcajada, P., & Vallet-Regí, M. (2006). Confinement and controlled release of bisphosphonates on ordered mesoporous silica-based materials. *Journal of the American Chemical Society*, 128(25), 8116–8117. doi:10.1021/ja062286z
  10. Bariana, M., Aw, M. S., Kurkuri, M., & Losic, D. (2013). Tuning drug loading and release properties of diatom silica microparticles by surface modifications. *International Journal of Pharmaceutics*, 443(1–2), 230–241.  
doi:10.1016/j.ijpharm.2012.12.012
  11. Barsanti, L., & Gualtieri, P. (2014). *Algae: Anatomy, biochemistry, and biotechnology*. Boca Raton Florida: CRC Press/Taylor & Francis Group.
  12. Beakes, G. W., Canter, H. M., & Jaworski, G. H. (1988). Zoospore ultrastructure of *zygorhizidium affluens* and *z. planktonicum*, two chytrids parasitizing the diatom *asterionella formosa*. *Canadian Journal of Botany*, 66(6), 1054–1067. doi:10.1139/b88-151

13. Cai, T., Park, S. Y., & Li, Y. (2013). Nutrient recovery from wastewater streams by microalgae: Status and prospects. *Renewable and Sustainable Energy Reviews*, *19*, 360–369. doi:10.1016/j.rser.2012.11.030
14. Cicco, S. R., Vona, D., De Giglio, E., Cometa, S., Mattioli-Belmonte, M., Palumbo, F., ... Farinola, G. M. (2015). Chemically modified diatoms Biosilica for bone cell growth with combined drug-delivery and antioxidant properties. *ChemPlusChem*, *80*(7), 1104–1112. doi:10.1002/cplu.201402398
15. Collos, Y., & Slawyk, G. (1980). Nitrogen uptake and assimilation by marine phytoplankton. *Primary Productivity in the Sea*, 195–211. doi:10.1007/978-1-4684-3890-1\_11
16. Delalat, B., Sheppard, V. C., Rasi Ghaemi, S., Rao, S., Prestidge, C. A., McPhee, G., ... Voelcker, N. H. (2015). Targeted drug delivery using genetically engineered diatom biosilica. *Nature Communications*, *6*(1). doi:10.1038/ncomms9791
17. Denny, P., Cren, E. D., & Lowe-McConnell, R. H. (1981). The functioning of freshwater ecosystems. *The Journal of Ecology*, *69*(2), 718. doi:10.2307/2259702
18. Dissolved oxygen and biochemical oxygen demand. (2012). Environmental Protection Agency. Retrieved from <https://archive.epa.gov/water/archive/web/html/vms52.html>
19. Eddy, F. B., & Williams, E. M. (1987). Nitrite and freshwater fish. *Chemistry and Ecology*, *3*(1), 1–38. doi:10.1080/02757548708070832

20. García, J., Mujeriego, R., & Hernández-Mariné, M. (2000). High rate algal pond operating strategies for urban wastewater nitrogen removal. *Journal of Applied Phycology*, *12*(3/5), 331–339. doi:10.1023/a:1008146421368
21. Gardner, R. C., & Davidson, N. C. (2011). The Ramsar convention. *Wetlands*, 189–203. doi:10.1007/978-94-007-0551-7\_11
22. Gnanamoorthy, P., Anandhan, S., & Prabu, V. A. (2014). Natural nanoporous silica frustules from marine diatom as a biocarrier for drug delivery. *Journal of Porous Materials*, *21*(5), 789–796. doi:10.1007/s10934-014-9827-2
23. Goa State Biodiversity Board. (2020). Batim Lake. [https://gsbb.goa.gov.in/wp-content/uploads/2020/11/9.-Batim\\_Lake-NIO-BD.pdf](https://gsbb.goa.gov.in/wp-content/uploads/2020/11/9.-Batim_Lake-NIO-BD.pdf)
24. González, L. E., Cañizares, R. O., & Baena, S. (1997). Efficiency of ammonia and phosphorus removal from a Colombian agroindustrial wastewater by the microalgae *Chlorella vulgaris* and *Scenedesmus dimorphus*. *Bioresource Technology*, *60*(3), 259–262. doi:10.1016/S0960-8524(97)00029-1
25. Grasshoff, K., Kremling, K., Ehrhardt, M., & Anderson, L. G. (1999). *Methods of seawater analysis*. Weinheim, Germany: Wiley-VCH.
26. Guillard, R. R., & Ryther, J. H. (1962). Studies of marine planktonic diatoms: I. *Cyclotella nana* Hustedt, and *Detonula confervacea* (Cleve) Grun. *Canadian Journal of Microbiology*, *8*(2), 229–239. doi:10.1139/m62-029
27. Guillard, R. R. (1975). Culture of phytoplankton for feeding marine invertebrates. *Culture of Marine Invertebrate Animals*, 29–60. doi:10.1007/978-1-4615-8714-9\_3

28. Gürel, A., & Yıldız, A. (2007). Diatom communities, lithofacies characteristics and Paleoenvironmental interpretation of Pliocene diatomite deposits in the İhlara–selime plain (Aksaray, Central Anatolia, Turkey). *Journal of Asian Earth Sciences*, 30(1), 170–180. doi:10.1016/j.jseaes.2006.07.015
- Hasle, G. R., & Tomas, C. R. (1997). *Identifying marine phytoplankton*. San Diego U.S.A.: Acad. Press.
29. Hd., J., & Odum, E. P. (1974). *Fundamentals of Ecology. Population* (French Edition), 29(2), 376. doi:10.2307/1530838
30. Hindarti, D., & Larasati, A. W. (2019). Copper (Cu) and cadmium (Cd) toxicity on growth, chlorophyll-a and carotenoid content of phytoplankton *Nitzschia* sp.. IOP Conference Series: Earth and Environmental Science, 236, 012053. doi:10.1088/1755-1315/236/1/012053
31. Jeppesen, E., Peder Jensen, J., Søndergaard, M., Lauridsen, T., Junge Pedersen, L., & Jensen, L. (1997). Top-down control in freshwater lakes: The role of nutrient state, submerged macrophytes and water depth. *Shallow Lakes '95*, 151–164. doi:10.1007/978-94-011-5648-6\_17
32. Jiang, W., Luo, S., Liu, P., Deng, X., Jing, Y., Bai, C., & Li, J. (2013a). Purification of biosilica from living diatoms by a two-step acid cleaning and baking method. *Journal of Applied Phycology*, 26(3), 1511–1518. doi:10.1007/s10811-013-0192-3
33. Ketchum, B. H., & Hutchinson, G. E. (1958). A treatise on limnology, vol. I. Geography, physics and Chemistry. *AIBS Bulletin*, 8(2), 47. doi:10.2307/1291951

34. Kilham, P., & Hecky, R. E. (1988). Comparative ecology of marine and Freshwater Phytoplankton1. *Limnology and Oceanography*, 33(4part2), 776–795. doi:10.4319/lo.1988.33.4part2.0776
35. Kong, Q., Li, L., Martinez, B., Chen, P., & Ruan, R. (2009). Culture of microalgae chlamydomonas reinhardtii in wastewater for biomass feedstock production. *Applied Biochemistry and Biotechnology*, 160(1), 9–18. doi:10.1007/s12010-009-8670-4
36. Kumeria, T., Bariana, M., Altalhi, T., Kurkuri, M., Gibson, C. T., Yang, W., & Losic, D. (2013). Graphene oxide decorated diatom silica particles as new nano-hybrids: Towards Smart Natural Drug Microcarriers. *Journal of Materials Chemistry B*, 1(45), 6302. doi:10.1039/c3tb21051k
37. Lavoie, A., & de la Noüe, J. (1985). Hyperconcentrated cultures of Scenedesmus Obliquus. *Water Research*, 19(11), 1437–1442. doi:10.1016/0043-1354(85)90311-2
38. Lim, H., Seo, Y., Kwon, D., Kang, S., Yu, J., Park, H., ... Lee, T. (2023). Recent progress in diatom Biosilica: A natural nanoporous silica material as sustained release carrier. *Pharmaceutics*, 15(10), 2434. doi:10.3390/pharmaceutics15102434
39. Litchman, E., Klausmeier, C. A., Miller, J. R., Schofield, O. M., & Falkowski, P. G. (2006). Multi-nutrient, multi-group model of present and future oceanic phytoplankton communities. *Biogeosciences*, 3(4), 585–606. doi:10.5194/bg-3-585-2006
40. Losic, D., Yu, Y., Aw, M. S., Simovic, S., Thierry, B., & Addai-Mensah, J. (2010). Surface functionalisation of diatoms with dopamine modified iron-

- oxide nanoparticles: Toward magnetically guided drug microcarriers with biologically derived morphologies. *Chemical Communications*, 46(34), 6323. doi:10.1039/c0cc01305f
41. Lv, J., Liu, Y., Feng, J., Liu, Q., Nan, F., & Xie, S. (2018). Nutrients removal from undiluted cattle farm wastewater by the two-stage process of microalgae-based wastewater treatment. *Bioresource Technology*, 264, 311–318. doi:10.1016/j.biortech.2018.05.085
42. Maher, S., Kumeria, T., Aw, M. S., & Losic, D. (2018). Diatom silica for biomedical applications: Recent progress and advances. *Advanced Healthcare Materials*, 7(19). doi:10.1002/adhm.201800552
43. Mancera-Andrade, E. I., Parsaeimehr, A., Ruiz-Ruiz, F., Rorrer, G. L., González-Valdez, J., Iqbal, H. M. N., & Parra-Saldivar, R. (2019). Isorhamnetin encapsulation into biogenic silica from cyclotella sp.. using a microfluidic device for drug delivery applications. *Biocatalysis and Agricultural Biotechnology*, 19, 101175. doi:10.1016/j.bcab.2019.101175
44. Marella, T. K., Parine, N. R., & Tiwari, A. (2018). Potential of diatom consortium developed by nutrient enrichment for biodiesel production and simultaneous nutrient removal from wastewater. *Saudi Journal of Biological Sciences*, 25(4), 704–709. doi:10.1016/j.sjbs.2017.05.011
45. Martin-Jézéquel, V., Hildebrand, M., & Brzezinski, M. A. (2000). Silicon metabolism in diatoms: Implications for growth. *Journal of Phycology*, 36(5), 821–840. doi:10.1046/j.1529-8817.2000.00019.x
46. Martínez, M. E., Jiménez, J. M., & El Yousfi, F. (1999). Influence of phosphorus concentration and temperature on growth and phosphorus uptake

- by the microalga *scenedesmus obliquus*. *Bioresource Technology*, 67(3), 233–240. doi:10.1016/s0960-8524(98)00120-5
47. McInnes, S. J., & Voelcker, N. H. (2009). Silicon–polymer hybrid materials for drug delivery. *Future Medicinal Chemistry*, 1(6), 1051–1074. doi:10.4155/fmc.09.90
48. Mulbry, W., Kondrad, S., Pizarro, C., & Kebede-Westhead, E. (2008). Treatment of dairy manure effluent using freshwater algae: Algal productivity and recovery of manure nutrients using pilot-scale algal turf scrubbers. *Bioresource Technology*, 99(17), 8137–8142. doi:10.1016/j.biortech.2008.03.073
49. Narayan, R., Nayak, U., Raichur, A., & Garg, S. (2018). Mesoporous silica nanoparticles: A comprehensive review on synthesis and recent advances. *Pharmaceutics*, 10(3), 118. doi:10.3390/pharmaceutics10030118
50. Nasser, K. M. M. (2013). *Ecology and Biodiversity of Freshwater Microalgae in the Selected Areas of the Western Ghats* (thesis). Retrieved from <http://hdl.handle.net/10603/30556>
51. Phogat, S., Saxena, A., Kapoor, N., Aggarwal, C., & Tiwari, A. (2021). Diatom mediated Smart Drug Delivery System. *Journal of Drug Delivery Science and Technology*, 63, 102433. doi:10.1016/j.jddst.2021.102433
52. Qi, Y., Wang, X., & Cheng, J. J. (2016). Preparation and characteristics of biosilica derived from marine diatom biomass of *Nitzschia Closterium* and *Thalassiosira*. *Chinese Journal of Oceanology and Limnology*, 35(3), 668–680. doi:10.1007/s00343-017-5329-9

53. Quinn, P. K., Asher, W. E., & Charlson, R. J. (1992). Equilibria of the marine multiphase ammonia system. *Journal of Atmospheric Chemistry*, 14(1–4), 11–30. doi:10.1007/bf00115219
54. Rabiee, N., Khatami, M., Jamalipour Soufi, G., Fatahi, Y., Irvani, S., & Varma, R. S. (2021). Diatoms with invaluable applications in nanotechnology, biotechnology, and biomedicine: Recent advances. *ACS Biomaterials Science & Engineering*, 7(7), 3053–3068. doi:10.1021/acsbiomaterials.1c00475
55. Rajawat, M. V., Singh, S., & Saxena, A. K. (2014). A new spectrophotometric method for quantification of potassium solubilized by bacterial cultures. *Indian journal of experimental biology*, 52(3), 261–266.
56. Rayne, N., & Aula, L. (2020). Livestock manure and the impacts on Soil Health: A Review. *Soil Systems*, 4(4), 64. doi:10.3390/soilsystems4040064
57. Rodrigues, B. F., & Sawaiker, R. U. (2016). Physico-chemical characteristics and phytoplankton diversity in some freshwater bodies of Goa, India. *Journal of Environmental Research And Development*, 10(4). Ryland, D. (1994). The European Environment Agency. *European Energy and Environmental Law Review*, 3(Issue 5), 138–140. doi:10.54648/eelr1994023
58. Saad, E. M., Pickering, R. A., Shoji, K., Hossain, M. I., Glover, T. G., Krause, J. W., & Tang, Y. (2020). Effect of cleaning methods on the dissolution of diatom frustules. *Marine Chemistry*, 224, 103826. doi:10.1016/j.marchem.2020.103826

59. Sardo, A., Orefice, I., Balzano, S., Barra, L., & Romano, G. (2021). Mini-Review: Potential of diatom-derived silica for biomedical applications. *Applied Sciences*, *11*(10), 4533. doi:10.3390/app11104533
60. Schindler, D. W. (1978). Factors regulating phytoplankton production and standing crop in the world's freshwaters. *Limnology and Oceanography*, *23*(3), 478–486. doi:10.4319/lo.1978.23.3.0478
61. Seaborn, D. W., & Wolny, J. L. (2000). Scanning electron microscopy. *Methods in Plant Electron Microscopy and Cytochemistry*, 185–194. doi:10.1007/978-1-59259-232-6\_13
62. Sheng, G., Wang, S., Hu, J., Lu, Y., Li, J., Dong, Y., & Wang, X. (2009). Adsorption of pb(ii) on diatomite as affected via aqueous solution chemistry and temperature. *Colloids and Surfaces A: Physicochemical and Engineering Aspects*, *339*(1–3), 159–166. doi:10.1016/j.colsurfa.2009.02.016
63. Simovic, S., Ghouchi-Eskandar, N., Moom Sinn, A., Losic, D., & A. Prestidge, C. (2011). Silica materials in drug delivery applications. *Current Drug Discovery Technologies*, *8*(3), 250–268. doi:10.2174/157016311796799026
64. Sournia, A. (1978). *Phytoplankton manual*. Paris: Unesco.
65. Spivakov, B. Ya., Maryutina, T. A., & Muntau, H. (1999). Phosphorus speciation in water and sediments. *Pure and Applied Chemistry*, *71*(11), 2161–2176. doi:10.1351/pac199971112161
66. *Standard test methods for ammonia nitrogen in water*. (2008). West Conshohocken, PA: Dodds, W. K., Bouska, W. W., Eitzmann, J. L., Pilger, T. J., Pitts, K. L., Riley, A. J., ... Thornbrugh, D. J. (2008). Eutrophication

- of U.S. freshwaters: Analysis of potential economic damages. *Environmental Science & Technology*, 43(1), 12–19. doi:10.1021/es801217q
67. Sturm, B. S. M., & Lamer, S. L. (2011). An energy evaluation of coupling nutrient removal from wastewater with algal biomass production. *Applied Energy*, 88(10), 3499–3506. doi:10.1016/j.apenergy.2010.12.056
68. Terracciano, M., Shahbazi, M.-A., Correia, A., Rea, I., Lamberti, A., De Stefano, L., & Santos, H. A. (2015). Surface bioengineering of diatomite based nanovectors for efficient intracellular uptake and drug delivery. *Nanoscale*, 7(47), 20063–20074. doi:10.1039/c5nr05173h
69. Townsend, M. G. V. (1993). *The Ramsar convention on wetlands: Its history and development*. Gland: Ramsar Convention Bureau.
70. Tripathi, S. P. M., Pathak, M., & Tiwari, J. P. (2008). A study on organic pollution based on algal distribution in some rural and temple ponds of Balrampur, U.P. India. *Environment Conservation Journal*, 9(3), 61–64. doi:10.36953/ecj.2008.090313
71. Ukmar, T., Maver, U., Planinšek, O., Kaučič, V., Gabersček, M., & Godec, A. (2011). Understanding controlled drug release from mesoporous silicates: Theory and experiment. *Journal of Controlled Release*, 155(3), 409–417. doi:10.1016/j.jconrel.2011.06.038
72. Umemura, K., Noguchi, Y., Ichinose, T., Hirose, Y., Kuroda, R., & Mayama, S. (2008). Diatom cells grown and baked on a functionalized mica surface. *Journal of Biological Physics*, 34(1–2), 189–196. doi:10.1007/s10867-008-9086-z
73. Wang, L., Li, Y., Chen, P., Min, M., Chen, Y., Zhu, J., & Ruan, R. R. (2010). Anaerobic digested dairy manure as a nutrient supplement for cultivation of

- oil-rich green microalgae chlorella sp... *Bioresource Technology*, 101(8), 2623–2628. doi:10.1016/j.biortech.2009.10.062
74. Wang, X.-W., Huang, L., Ji, P.-Y., Chen, C.-P., Li, X.-S., Gao, Y.-H., & Liang, J.-R. (2019). Using a mixture of wastewater and seawater as the growth medium for wastewater treatment and lipid production by the marine Diatom *Phaeodactylum Tricornutum*. *Bioresource Technology*, 289, 121681. doi:10.1016/j.biortech.2019.121681
75. Wang, Y., Cai, J., Jiang, Y., Jiang, X., & Zhang, D. (2012). Preparation of biosilica structures from frustules of diatoms and their applications: Current State and Perspectives. *Applied Microbiology and Biotechnology*, 97(2), 453–460. doi:10.1007/s00253-012-4568-0
76. Wetzel, R. G., & Likens, G. E. (2000). Dissolved oxygen. *Limnological Analyses*, 73–84. doi:10.1007/978-1-4757-3250-4\_6
77. Wilhm, J., & Dorris, T. (1968). Biological parameters for water quality criteria. *BioScience*, 18(6), 477–481. doi:10.2307/1294272
78. Wilkie, A. (2002). Recovery of dairy manure nutrients by benthic freshwater algae. *Bioresource Technology*, 84(1), 81–91. doi:10.1016/s0960-8524(02)00003-2
79. Xu, X., Chen, M., Yang, G., Jiang, B., & Zhang, J. (2020). Wetland Ecosystem Services Research: A critical review. *Global Ecology and Conservation*, 22. doi:10.1016/j.gecco.2020.e01027
80. Zhou, W., Min, M., Li, Y., Hu, B., Ma, X., Cheng, Y., ... Ruan, R. (2012). A hetero-photoautotrophic two-stage cultivation process to improve

wastewater nutrient removal and enhance algal lipid accumulation.  
*Bioresource Technology*, 110, 448–455. doi:10.1016/j.biortech.2012.01.063

## APPENDICES

### Media preparation:

#### 1. f/2 medium (Guillard and Ryther 1962, Guillard 1975).

All the stock components must be stored at <4 °C. Additionally, the vitamin stock solution and trace metal solution have to be filter-sterilised prior to

<b>Component</b>	<b>Stock solution</b>	addition into the final medium.
NaNO <sub>3</sub>	75 g/L dH <sub>2</sub> O	
NaHPO <sub>4</sub> .H <sub>2</sub> O	5 g/L dH <sub>2</sub> O	
Na <sub>2</sub> SiO <sub>3</sub> .9H <sub>2</sub> O	30 g/L dH <sub>2</sub> O	
Trace metal solution	-	
Vitamin solution	-	

#### Preparation of Trace Metal solution:

<b>Component</b>	<b>Primary Stock Solution</b>
FeCl <sub>3</sub> .6H <sub>2</sub> O	---
Na <sub>2</sub> EDTA.2H <sub>2</sub> O	---
CuSO <sub>4</sub> .5H <sub>2</sub> O	9.8 g/L dH <sub>2</sub> O
Na <sub>2</sub> MoO <sub>4</sub> .2H <sub>2</sub> O	6.3 g/L dH <sub>2</sub> O
ZnSO <sub>4</sub> .7H <sub>2</sub> O	22.0 g/L dH <sub>2</sub> O
CoCl <sub>2</sub> .6H <sub>2</sub> O	10.0 g/L dH <sub>2</sub> O
MnCl <sub>2</sub> .4H <sub>2</sub> O	180.0 g/L dH <sub>2</sub> O

#### Preparation of Vitamin solution:

<b>Component</b>	<b>Primary Stock Solution</b>
thiamine HCl (vit. B <sub>1</sub> )	---
biotin (vit. H)	0.1 g/L dH <sub>2</sub> O
cyanocobalamin (vit. B <sub>12</sub> )	1.0 g/L dH <sub>2</sub> O

### **Reagent preparation:**

#### **1. Lugol's Iodine (Himedia, S019).**

<b>Ingredients</b>	<b>Quantity</b>
Iodine	5 g
Potassium iodide	10 g
Distilled water	100 mL

#### **2. Estimation of Phosphates (Grasshoff et al., 1999):**

- a. Sulphuric acid (Reagent 1) - Carefully add 250 mL of concentrated sulphuric acid to 750 mL of pure water. Allow to cool and dilute to 1 L. Store in a polyethylene bottle.
- b. Phosphate standard solution: 136.09 mg of Potassium dihydrogen phosphate,  $\text{KH}_2\text{PO}_4$ , is dissolved in distilled water to which has been added 0.2 mL of sulphuric acid (reagent 1) and made up to 100 mL. Store cold in a glass bottle the solution is stable for months. This standard stock solution contains 10 mmol/L phosphate.
- c. Ascorbic acid solution: Dissolve 10 g of ascorbic acid in 50 mL of distilled water, then add 50 mL of sulphuric acid (reagent 1) and store in dark in a brown bottle at  $< 8\text{ }^\circ\text{C}$ , the reagent is stable for several weeks as long as it remains colourless.
- d. Mixed reagent: Dissolve 12.5 g of ammonium heptamolybdate tetrahydrate in 125 mL of distilled water. Also dissolve 0.5 g of potassium antimony tartrate in 20 mL of pure water. Add the molybdate solution to 350 mL of sulphuric acid (reagent 1) while continuously stirring. Add the tartrate

solution and mix well. Store in a laboratory glass bottle. This mixed reagent is stable for several months.

### **3. Estimation of Silicates (Grasshoff et al., 1999):**

- a. Acid molybdate reagent: Dissolve 38 g of ammonium heptamolybdate tetrahydrate, in 300 mL of distilled water. Add this solution to 300 mL of sulphuric acid (reagent 1). Do not add acid to molybdate. If stored protected from direct sunlight, the reagent is stable for several months.
- b. Oxalic acid solution: Dissolve 10 g of oxalic acid dihydrate in 100 ml of distilled water. Store this saturated solution in a plastic bottle at room temperature. It is stable indefinitely.
- c. Ascorbic acid solution: Dissolve 2.8 g of ascorbic acid in 100 mL of pure water. Store in an amber glass bottle at  $< 8^{\circ}\text{C}$ . The reagent is effective as long as it remains colourless.
- d. Standard stock solution: Add 5.188 mg of hexafluorosilicate in 100 mL of distilled water in a plastic beaker. This solution contains 10 mmol/L. The standard is stable for at least one year.

### **4. Estimation of Nitrite (Grasshoff et al., 1999):**

- a. Sulphanilamide: 10 g of crystalline sulphanilamide are dissolved in 100 mL of concentrated hydrochloric acid in about 600 mL of distilled water. After cooling, the solution is made up to 1 L with distilled water. Store in the dark at  $< 8^{\circ}\text{C}$ . The reagent is stable for at least one month.
- b. N-(1 -naphthyl)-ethylenediamine dihydrochloride: 0.5 g of the amine dihydrochloride is dissolved in 500mL of pure water. The solution should be

stored in a brown bottle at  $< 8^{\circ}\text{C}$ . The reagent is stable for more than a month and can be used until a brown discolouration occurs.

- c. Nitrite standard solution: 0.690 g of Anhydrous sodium nitrite ( $\text{NaNO}_2$ ) is dissolved in 1 L of distilled water. The solution contains 10 mmol/L of nitrite and should be stored cool and dark place.

#### **5. Estimation of Dissolved Oxygen (Grasshoff et al., 1999):**

- a. Manganese (II) chloride (Winkler's A): 60 g of  $\text{MnCl}_2 \cdot 4\text{H}_2\text{O}$  are dissolved and made up to 100 mL with distilled water.
- b. Alkaline iodide (Winkler's B): 60 g of KI and 30 g of KOH are dissolved separately in a minimum amount of water and combined. The solution is made up to 100 mL with distilled water, and stored in an amber-coloured bottle.
- c. Sulphuric acid: 50mL of concentrated sulphuric acid are added carefully to 50mL of distilled water (the mixture must be cooled while mixing).
- d. Sodium thiosulphate, 0.2 mol/L: 49.5 g of  $\text{Na}_2\text{S}_2\text{O}_3 \cdot 5\text{H}_2\text{O}$  are dissolved and made up to 1 L with distilled water.
- e. Sodium thiosulphate, 0.02 mol/L: The 0.02 mol/L working solution is a 1 : 10 dilution of 0.2 mol/l sodium thiosulphate solution.
- f. Starch solution: 1 g of soluble starch is dispersed in 100 mL of distilled water. The solution is quickly heated to boiling point. Use only freshly prepared solution for estimation.

#### **6. Determination of Nitrate (Grasshoff et al., 1999):**

- a. Ammonium chloride buffer: 10 g of ammonium chloride are dissolved in 1 L of distilled water. The pH is adjusted to 8.5 with about 1.5 mL of 25 % ammonia solution.
- b. Reductor filling: Commercially available granulated cadmium (e.g., Merck) is sieved and the fraction between 40 and 60 mesh is retained and used.
- c. Copper sulphate: 1 g of copper sulphate pentahydrate ( $\text{CuSO}_4 \cdot 5\text{H}_2\text{O}$ ) is dissolved in about 100 mL of distilled water.
- d. Nitrate standard solution: 1.011 g of dry potassium nitrate ( $\text{KNO}_3$ ) is dissolved and made up to 1 L with distilled water. The stock solution contains 10 mmol/L nitrate and is stable.